UNIVERSITY OF TURKU

Development of VCl_3-free synthetic routes for MIL-100(V) and its application in heterogeneous catalysis

MSc Chemistry

Master's thesis

Sanele Sibanda

15.05.2026

Turku

Master's thesis

Subject: Chemistry of Materials for Sustainable Development

Author: Sanele Sibanda

Title: Development of VCl_3-free synthetic routes for MIL-100(V) and its application in heterogeneous catalysis

Supervisor: Docent Ari Lehtonen

Number of pages: 56 pages

Date: 15.05.2026

This research investigates the development of sustainable, VCl_3-free synthetic routes for vanadium-containing MIL-100 metal-organic frameworks. Traditional VCl_3-based synthesis methods pose significant environmental and safety concerns due to the hazardous nature of the precursor. This study explores alternative vanadium sources, namely $VOSO_4 \cdot 5H_2O$, $V(acac)_3$, and V_2O_5, through both direct solvothermal synthesis and bimetallic synthesis strategies.

Material characterization was performed using powder X-ray diffraction, Fourier-transform infrared spectroscopy, thermogravimetric analysis, and X-ray fluorescence spectroscopy to evaluate crystallinity, structural stability, and elemental composition. Results reveal that direct synthesis routes typically yield materials with low crystallinity or phase impurities. In contrast, bimetallic synthesis of vanadium containing MIL-100(Fe) and MIL-100(Al) frameworks successfully preserves the characteristic MIL-100 topology while incorporating vanadium into the structure.

Catalytic evaluations using tert-butyl hydroperoxide as oxidant demonstrate that vanadium-incorporated MIL-100 materials exhibit redox activity in the oxidation of diverse substrates, including *cis*-cyclooctene, thioanisole, benzyl alcohol, and benzoin. Complete conversion was achieved for benzoin oxidation, while other substrates showed partial conversion.

The study concludes that vanadium-incorporated MIL-100 materials are promising catalysts for redox-mediated transformations, though catalytic efficiency depends critically on the uniformity and accessibility of active sites within the framework. While bimetallic synthesis strategies overcome synthesis barriers associated with direct crystallization, maintaining long-range order remains a critical challenge for optimizing the performance of vanadium-based MIL-100 frameworks in catalytic applications.

Keywords: metal-organic frameworks, sustainable synthesis, heterogeneous catalysis, oxidation reactions.

List of Acronyms

Acronym	Full form
DMF	N,N-Dimethylformamide
FTIR	Fourier-Transform Infrared
MIL	Materials of Institut Lavoisier
MOF	Metal Organic Frameworks
NMR	Nuclear Magnetic Resonance
PXRD	Powder X-Ray Diffraction
Tert-BuOOH	tert-butyl hydroperoxide
TGA	Thermogravimetric Analysis
XRF	X-Ray Fluorescence

Table of contents

1 Introduction

1.1 Metal-organic frameworks

Metal-organic frameworks (MOFs) are crystalline porous materials constructed from inorganic metal nodes and organic linkers connected through coordinate bonds.[1,2] They exhibit exceptionally high surface areas, well-defined pore structures, and chemical versatility, making them excellent candidates for applications in gas storage, adsorbents, sensing, drug delivery, heterogeneous catalysis and energy storage.[3–5]

The synthesis of MOFs is governed by numerous parameters, including temperature, the choice of metal ion, the identity of the organic linker, the solvent environment, and the possible presence of counterions. The pore size and architecture of MOFs can be influenced by adjusting the length and functional groups of the organic linker and the coordination geometry of the metal centre, for example, octahedral, square planar, or tetrahedral. Typical metals used in MOF synthesis include first-row transition metals, lanthanides, and alkaline earth metals.[3] Figure 1 shows an example of a MOF built from Zn_4O clusters and benzene-1,4-dicarboxylate linkers.

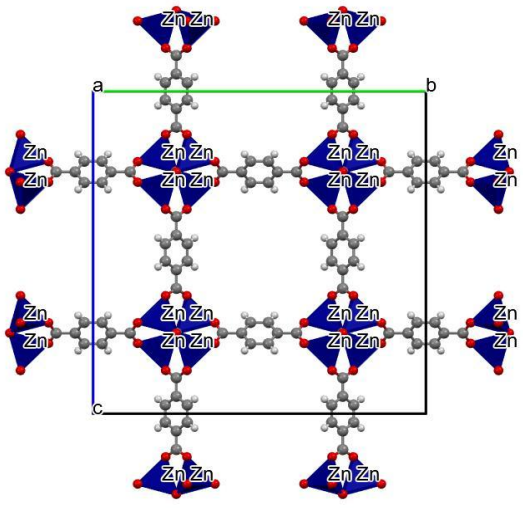

Figure 1 IRMOF, a metal-organic framework made from Zn_4O cluster and 1,4-benzo dicarboxylic acid adapted from Eddaoudi et al.[6]

The rational design of MOFs requires a fundamental understanding of metal-ligand coordination chemistry, crystal nucleation and growth kinetics, and the thermodynamic stability of the resulting framework structures. The choice of metal centre is particularly critical, as it determines not only the coordination geometry and connectivity of the inorganic nodes but also the electronic properties, redox behaviour, and catalytic activity of the resulting material.[7]

Modulators such as monocarboxylic acids, for example acetic acid, or bases, such as triethylamine or sodium hydroxide, are frequently employed to control the deprotonation kinetics of the organic linker and to compete with the linker for metal coordination sites. This can slow crystal growth and improve crystallinity.[8] Mineralizing agents such as HF can also enhance the crystallinity of certain MOF families by promoting dissolution and recrystallization of amorphous precursors and stabilizing specific metal-oxo cluster geometries.[9,10] However, HF poses significant safety and environmental concerns, motivating the development of HF-free synthesis routes that can achieve comparable structural quality through alternative strategies such as mechanochemical synthesis, microwave-assisted heating, or post-synthetic modification.[11,12]

1.2 MIL-100

Among early mesoporous MOFs, the MIL-100 series (MIL: Materials of Institut Lavoisier), first reported by Férey and co-workers, is distinguished by its large mesoporous cages and accessible metal sites.[2,7] The MIL-100 structure is made of trivalent metal ions and trimeric metal-oxo clusters coordinated by 1,3,5-benzene tricarboxylic (BTC) acid linkers, forming large cages accessible through microporous windows. Their architecture enables exceptional adsorption, catalytic activity, and molecular encapsulation, positioning MIL-100 MOFs as key materials in environmental, catalytic and separation technologies.[2,7]

The MIL-100 topology is defined by a cubic crystal system and is categorized under the Fd-3m space group. This arrangement results in a hierarchical pore structure that comprises two distinct types of mesoporous cages. The smaller cages possess free diameters of approximately 25 Å and are typically accessible through pentagonal

windows with dimensions of roughly 5.5 Å. In contrast, the larger cages feature internal diameters of approximately 29 Å. These larger voids are accessible through a combination of pentagonal and hexagonal windows, with the hexagonal windows providing a larger aperture of approximately 8.6 Å as depicted in Figure 2.[13]

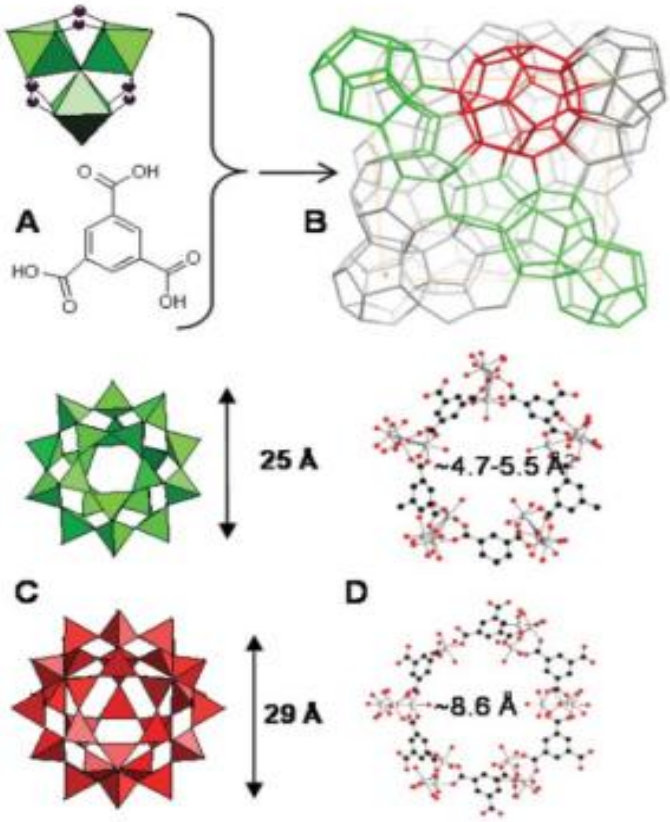

Figure 2 Structure of MIL-100(Fe) published by Horcajada et al.[13] (A) The metal cluster and BTC acid precursors. (B) one unit cell of MIL-100(Fe). (C) a representation of the cages as polyhedra. (D) A ball and stock model of the pentagonal and hexagonal windows.

This dual-cage architecture facilitates the molecular encapsulation and selective diffusion of various substrates within the framework, with the smaller windows restricting access to bulky molecules while allowing the diffusion of smaller substrates and products.[13] The trimeric metal-oxo clusters that constitute the inorganic nodes of the MIL-100 framework feature coordinatively unsaturated metal sites that can be generated by thermal activation or solvent removal, providing Lewis acidic centre that are highly active for catalytic transformations.[14]

The structural stability of MIL-100 materials is intimately linked to the nature of the trivalent metal centre. Computational and experimental studies have shown that the

binding energy of the benzene tricarboxylate linker to the trimeric metal cluster, as well as the thermodynamic stability of the oxo bridge, varies significantly across different metals.[15] Metals such as Cr and Fe, which form highly stable octahedral coordination environments and exhibit strong metal-oxygen bonds, tend to produce MIL-100 frameworks with exceptional thermal and chemical stability.[16] In contrast, metals with more labile coordination spheres or those prone to redox chemistry under synthesis conditions may yield frameworks with lower crystallinity or reduced stability.[17]

The synthesis of MIL-100 materials typically involves the reaction of a trivalent metal salt, such as $FeCl_3$, $Cr(NO_3)_3$, or $Al(NO_3)_3$, with BTC acid in aqueous or mixed solvent systems at temperatures ranging from 100 to 220 °C.[18] The use of HF as a mineralizing agent has been shown to be particularly effective for promoting the formation of highly crystalline MIL-100(Cr) and MIL-100(Fe), with the fluoride anion believed to stabilize the trimeric metal-oxo cluster and facilitate dissolution and recrystallization of poorly ordered precursor phases. However, recent HF-free approaches have shown that comparable crystallinity can sometimes be achieved through careful control of pH, temperature, and reaction time, often with post-synthetic solvent exchange or thermal annealing.[11]

1.3 Applications of MIL-100 MOFs

Several metal variants of the MIL-100 structure have been reported, including MIL-100(Cr), MIL-100(Fe), MIL-100(Al) and MIL-100(V).[2] The identity of the metal centre imparts distinct properties to the MIL-100 framework. For example, MIL-100(Fe) has been widely studied for biomedical applications due to it biocompatibility and the low toxicity of iron, while MIL-100(Cr) is widely used in gas storage due to its large surface area and robust structure.[2] MIL-100(V) has emerged as a compelling material because of the redox flexibility of vanadium, the accessibility of its metal sites, and its structural similarity to the Fe and Cr analogues. The incorporation of vanadium introduces catalytic potential, especially for redox-driven transformations, while maintaining the characteristic hierarchical porosity of the MIL-100 topology.[19]

One of the most prominent applications of MIL-100 MOFs is adsorption and separation. Because of their large pore volumes and high surface areas, MIL-100 materials have

demonstrated strong performance in the adsorption of gases such as H_2, CO_2, CH_4 and H_2S, and the removal of environmentally hazardous pollutants from air and water. Fe-based MIL-100 exhibits notable affinity toward water vapour, CO_2 and toxic contaminants, making it a promising candidate for dehumidification, gas separation, and water purification technologies.[2,20–22]

The integration of CO_2 capture with its subsequent catalytic conversion into value-added chemicals is a significant research focus, particularly for mesoporous materials like the MIL-100 series. The open metal sites within the MIL-100 series act as Lewis acid centres that can activate CO_2 molecules, while the accessible porous structure facilitates the diffusion and retention of co-reactants such as epoxides or amines, enabling the synthesis of cyclic carbonates, carbamates, and other CO_2-derived products.[8,23]

The catalytic properties of MIL-100 materials are strongly influenced by the electronic structure and coordination chemistry of the metal centre. Studies comparing isomorphously substituted MIL-100(M) frameworks (M = Al, Cr, Fe, In, Sc, V) have revealed that the Lewis acidity, redox potential, and catalytic activity vary significantly across the series.[24] For example, in the Prins reaction, MIL-100(V) has been reported to exhibit superior activity compared with Fe, Al, and Cr analogues under identical conditions. This enhanced reactivity was attributed to the intermediate Lewis acidity of the vanadium centres, which is strong enough to activate the carbonyl group of the aldehyde but not so strong as to cause irreversible substrate binding or catalyst deactivation.[24]

Density functional theory calculations have provided mechanistic insights into the origin of these metal-dependent catalytic trends. The most effective catalytic performance occurs when metal centres possess intermediate binding energies, which allow them to facilitate both the activation of oxidants and the efficient release of the final oxidized products.[25] Vanadium is exceptionally well-suited for these roles because of its moderate oxophilicity and multiple accessible oxidation states, which grant the framework significant redox flexibility. This suggests that MIL-100(V) may be an effective platform for a wide variety of redox-mediated transformations.[25]

1.4 Challenges in MIL-100(V) synthesis

Despite the promising catalytic properties of vanadium-containing MIL-100 materials, the synthesis of phase-pure, highly crystalline MIL-100(V) remains significantly more challenging than that of the Fe, Cr, or Al analogues.[19,26] The first report of MIL-100(V) by Lieb et al. in 2012 used VCl_3 as the vanadium source and HF as a mineralizing agent, under hydrothermal conditions and produced a material consistent with the MIL-100 topology.[19] However, subsequent attempts to develop alternative routes using more readily available or less hazardous vanadium precursors have often resulted in low crystallinity, broad powder-x-ray diffraction (PXRD) peaks, or amorphous phases.[26,27]

The difficulties in synthesizing MIL-100(V) can be attributed to several factors related to the coordination chemistry and redox behaviour of vanadium. Vanadium exhibits rich redox chemistry, and the oxidation state required for MIL-100 formation is more difficult to maintain under many synthesis conditions.[28] Vanadium is also susceptible to oxidation and hydrolysis in the presence of oxygen or water, particularly at elevated temperatures, and the resulting species may not be compatible with the MIL-100 topology.[29]

Secondly, the hydrolysis and condensation kinetics of vanadium precursors differ significantly from those of Fe^{3+}, Cr^{3+}, or Al^{3+}. Vanadium salts such as $VOSO_4 \cdot 5H_2O$ undergo rapid hydrolysis in aqueous solution, forming a complex mixture of monomeric, dimeric, and oligomeric vanadium-oxo species whose speciation is highly sensitive to pH, temperature, and coordinating ligands. The formation of the trimeric vanadium-oxo cluster required for MIL-100 assembly therefore demands precise control, and deviations can lead to competing vanadium-oxide or hydroxide phases.[30]

Moreover, the choice of vanadium precursor has a strong influence on the synthesis outcome. VCl_3, which provides V^{3+} directly, is the most commonly used precursor for MIL-100(V) synthesis, but it is highly hygroscopic, air-sensitive, and expensive, limiting its practical use.[19] $VOSO_4 \cdot 5H_2O$, which contains V^{4+} as the vanadyl cation (VO^{2+}), is more stable and readily available, but may not readily produce the required clusters.[29]

Vanadium (III) acetylacetonate ($V(acac)_3$) is an attractive alternative that provides V^{3+} in a coordinatively saturated, air-stable form, but the acetylacetonate ligands must be displaced by the BTC acid linker during synthesis, and incomplete ligand exchange can lead to defective or poorly crystalline frameworks.[31]

Additionally, the role of mineralizing agents such as HF in promoting MIL-100(V) crystallinity is not fully understood. While HF is known to enhance the crystallinity of MIL-100(Fe) and MIL-100(Cr) by stabilizing the trimeric metal-oxo cluster and facilitating the dissolution and recrystallization of amorphous precursors[32], the specific interactions between fluoride anions and vanadium species under hydrothermal conditions are complex and may differ from those observed for Fe or Cr.[33] Moreover, the use of HF poses significant safety and environmental concerns, motivating the development of HF-free synthesis routes for MIL-100(V).[34]

Finally, the synthesis of MIL-100(V) is further complicated by the tendency of vanadium to form stable, crystalline vanadium oxide phases (e.g., V_2O_3, V_2O_5, VO_2) under hydrothermal or solvothermal conditions, particularly at high temperatures or in the presence of excess water.[35] These oxide phases are thermodynamically more stable than the kinetically controlled MOF phase, and their formation competes with MOF crystallization, often resulting in phase mixtures or the complete absence of the MIL-100 topology.[36] Strategies to suppress oxide formation include the use of lower synthesis temperatures, the addition of modulators or capping agents that preferentially bind to vanadium and prevent oxide nucleation, and the use of non-aqueous or mixed solvent systems that reduce the activity of water and shift the thermodynamic equilibrium in favour of the MOF phase.[37]

1.5 Bimetallic MOF synthesis

Given these challenges, alternative strategies for obtaining vanadium-containing MIL-100 materials have been explored. One approach is post-synthetic metal exchange. In this method, vanadium is introduced into a pre-formed MIL-100(Fe) or MIL-100(Al) framework by soaking the parent MOF in a solution of a vanadium salt. Another strategy is the direct co-synthesis of mixed-metal MIL-100(Fe, V) or MIL-100(Al, V) frameworks.[38,39] In this case, both metals are present in the initial synthesis mixture.

These approaches offer the advantage of leveraging the well-established synthesis protocols for MIL-100(Fe) or MIL-100(Al) while introducing vanadium in a controlled manner, potentially circumventing the crystallinity issues associated with direct MIL-100(V) synthesis.[40]

1.6 Objectives of this study

The primary objective of this study is to develop VCl_3-free synthesis routes to vanadium-containing MIL-100 materials using alternative vanadium precursors such as $VOSO_4 \cdot 5H_2O$ and $V(acac)_3$. Specific aims include investigating the influence of synthesis conditions on crystallinity and phase purity, exploring post-synthetic addition of vanadium and direct co-synthesis strategies, characterizing the resulting materials, and evaluating their catalytic activity in representative oxidation reactions.

By systematically exploring these synthesis strategies and establishing structure-property relationships, this work aims to provide a foundation for the rational design and scalable production of vanadium-based MIL-100 materials for catalytic applications.

2 Materials and methods

All chemicals used in this study were obtained from commercial suppliers and used without further purification. Powder X-ray Diffraction (PXRD) patterns were collected using a PANalytical diffractometer equipped with Cu Kα radiation (λ = 1.5406 Å) operating at 40 kV and 8 mA. X-ray fluorescence (XRF) spectroscopy through a PANalytical Epsilon 1 spectrometer was used to determine the elemental composition of the samples. Data were processed with the Omnian standardless analysis software, allowing semi-quantitative elemental determination without calibration standards. Fourier-transform infrared (FTIR) spectra were recorded on a Bruker spectrometer over the range 4000–400 cm^{-1}. For thermogravimetric analysis (TGA), a TA Instruments SDT Q600 simultaneous TGA–DSC analyser was used.

2.1 Synthesis of MIL-100(V)

2.1.1 Hydrothermal and solvothermal synthesis with $VOSO_4 \cdot 5H_2O$

$VOSO_4 \cdot 5H_2O$ (0.508 g, 2.00 mmol) was dissolved in N,N-dimethylformamide (DMF, 10.0 mL). In a separate beaker, BTC acid (0.211 g, 1.00 mmol) was dissolved in DMF (10.0 mL). The two solutions were combined in a 50.0 mL Teflon liner and a few drops of triethylamine were added. The Teflon liner was placed in an autoclave and heated at 130 ºC for 24 h. The product, VS1, was collected by suction filtration, washed with DMF, dried, and characterized by PXRD.

For hydrothermal synthesis, $VOSO_4 \cdot 5H_2O$ (0.506 g, 2.00 mmol) was dissolved in water (10.0 mL) and BTC acid (0.210 g, 1.00 mmol) was dissolved in water (10.0 mL). The two solutions were combined in a 50.0 mL Teflon liner and a few drops of triethylamine were added. The liner was sealed in an autoclave and heated at 130 °C for 24 h. The product, VS2, was collected by suction filtration, washed with water, dried, and characterised by PXRD.

2.1.2 Synthesis from vanadium(III) acetylacetonate

$V(acac)_3$ (0.112 g, 0.500 mmol) and BTC acid (0.102 g, 1.00 mmol) were dissolved in DMF (20.0 mL). The solution was heated in a 50.0 mL autoclave at 130 °C overnight. The product, VA1, was collected by suction filtration, washed with DMF, dried, and characterised by PXRD. A parallel synthesis of product VA2 was performed under reflux using the same quantities of precursors with an increased solvent volume of 30.0 mL.

2.1.3 Hydrothermal and solvothermal syntheses at pH 2

For synthesis in DMF: EtOH: H_2O (3: 1: 1, v/v), BTC acid (0.321 g, 1.50 mmol) was dissolved in DMF (7.20 mL). H_2O (2.40 mL) and EtOH (2.40 mL) were added, followed by $VOSO_4 \cdot 5H_2O$ (0.710 g, 3.00 mmol). The pH was adjusted to 2, and the solution was transferred to a 20.0 mL Teflon liner and heated in an autoclave at 120 °C for 24 h. A parallel synthesis was carried out at 130 °C for 48 h. The products, VS3 and VS4 respectively, were collected by suction filtration, washed with ethanol then water, and dried prior to PXRD characterisation.

For synthesis in EtOH: H_2O (1: 1, v/v), BTC acid (0.321 g, 1.50 mmol) was dissolved in EtOH (3.00 mL) at 50 °C with continuous stirring. A mixture of EtOH (6.00 mL) and H_2O (6.00 mL) was added, followed by $VOSO_4 \cdot 5H_2O$ (0.710 g, 3.00 mmol). After dissolution, the pH was adjusted to 2 and the mixture transferred to a 20.0 mL Teflon liner and heated at 120 °C for 24 h, with a parallel synthesis at 130 °C for 48 h. The products, VS5 and VS6 respectively, were washed with ethanol followed by water and dried before characterization by PXRD.

For hydrothermal synthesis, BTC acid (0.320 g, 1.5 mmol) was dissolved in 12 mL of H_2O then $VOSO_4 \cdot 5H_2O$ (0.71 g, 3 mmol) was stirred in with gentle heating. After complete dissolution of the precursors the pH of the resulting solution was adjusted to 2, then it was transferred to a 20.0 mL Teflon liner, placed in an autoclave and heated in an oven at 120 ºC for 24 h while a parallel synthesis was carried out at 130 ºC for 48 h. The products, VS7 and VS8 respectively, were collected by suction, washed with water, and dried before characterization by PXRD.

2.1.4 Solvothermal syntheses in the presence of HCl

The synthesis in DMF: ethanol: water (3:1:1) (v/v) was repeated without controlling the pH but with an addition of 1mL HCl (aq, 32.0 %) to the reaction mixture. The temperature of the synthesis was increased to 240 ºC and the duration was increased to 48 h, and the product VS9 was obtained.

2.1.5 Bimetallic MIL-100(Fe,V)

BTC acid (2.10 g, 10.0 mmol) was used for all syntheses. The Fe: V molar ratio was varied as shown below:

Table 1 Masses of Fe and V precursors used in synthesis

Ratio Fe: V	m($FeSO_4 \cdot 7H_2O$)/g	m($VOSO_4 \cdot 5H_2O$)/g	m(BTC acid)/g	Product name
1:2	2.78	5.06	2.10	BM12
1:3	2.09	5.69	2.10	BM13
1:4	1.67	6.07	2.10	BM14

BTC acid (2.10 g, 10.0 mmol) was dissolved in 1M NaOH (37.5 mL) using ultrasonic mixing to form solution A. In separate containers, each pair of metal precursors was dissolved in 40 mL of deionized water to form individual solutions B. Each solution B was added dropwise to its corresponding solution A at a rate of 2 mL min^{-1} using a constant-pressure separatory funnel at room temperature under continuous stirring. After complete addition, stirring was maintained for 24 h. The resulting products were collected by centrifugation and washed with ethanol followed by deionized water. The solids were dried under vacuum at 60 °C for 12 h prior to characterization by PXRD and XRF.

The synthesis at a metal-to-ligand ratio of 1:2 was repeated under ultrasonic mixing without changing the reagents to produce BM16. In parallel, synthesis of BM17 was performed in which 1M NaOH was replaced with 1M sodium acetate, while all other experimental conditions were kept constant.

For synthesis without Fe, BTC acid (0.420 g, 2.00 mmol) was dissolved in 1M NaOH (37.5 mL), and $VOSO_4 \cdot 5H_2O$ (1.52 g, 6.01 mmol) was dissolved in deionised water (40.0

mL). The metal solution was added dropwise to the ligand solution. The product, BM0, was processed as described above and characterised by PXRD, XRF and TGA.

2.1.6 Synthesis in the presence of HF

$VOSO_4 \cdot 5H_2O$ (5.66 g) and BTC acid (2.35 g) in water (20 mL) were stirred together with 1 mL of 5M HF at room temperature for 30 mins. The solution was then transferred to a 50.0 mL Teflon-lined autoclave and heated in an oven for 72 h at 220 ºC.

A parallel synthesis was run using V_2O_5 (4.07 g) and BTC acid (2,35 g) in 20 mL of water and 1 mL of 5M HF. The products, VS10 and VO1 respectively, of these syntheses were filtered off, washed with hot ethanol, dried under air at 100 ºC and characterised by PXRD.

2.1.7 Bimetallic MIL-100(Al,V)

MIL-100(Al,V) was prepared by combining two literature methods.[24,40] First MIL-100(Al) was prepared by mixing $Al(NO_3)_3 \cdot 9H_2O$ (1.74 g) with trimethyl- 1.3.5-benzenetricarboxylate (0.780 g) and 4M nitric acid (1.55 mL) in 25.2 mL of water. After adjusting the pH to 0.57, the mixture was heated at 160 ºC for 12 h. The product was collected by suction and dried at room temperature.

MIL-100(Al) was then doped with vanadium: $VOSO_4 \cdot 5H_2O$(1.17 g) was dissolved in 40 mL water and added dropwise to the obtained MIL-100(Al) suspended in water (37.5 mL) at 2.00 mL min^{-1} from a constant pressure separatory funnel with stirring. Stirring was continued for 24 hours at room temperature, then the product was collected by suction, washed subsequently with ethanol and water before being dried at room temperature. The product, BMAl, was characterized by PXRD and XRF.

2.2 Applications in heterogeneous catalysis

2.2.1 Catalytic addition of CO_2 to styrene oxide

The method for the catalytic addition of CO_2 to epoxides was adapted from literature.[23] V21 was activated by stirring in chloroform for 24 h (solvent replaced after 12 h) and

dried under vacuum at 80 °C overnight. The activated MOF (1.02 mg) was combined with styrene oxide (2.40 g, 20.0 mmol) and cocatalyst Bu_4NBr (1.12 mg) under a solvent-free CO_2 atmosphere created using a CO_2 balloon. The reaction was stirred at room temperature for 48 h and monitored by TLC.

2.2.2 Application of the MOFs in catalytic oxidation reactions

BM13, BM0 and BMAl were used for the oxidation reactions. Each MOF was activated separately by stirring in chloroform for 24 h (changing the solvent halfway through) then heating under a vacuum at 80 ºC overnight. Cis-cyclooctene (0.111 g. 1.00 mmol), thioanisole (0.124 g, 1.00 mmol) and benzyl alcohol (0.108g, 1.00 mmol) were separately reacted with tert-BuOOH (1.50 mmol) in dichloroethane (1.00 mL) and MOF catalyst (10.0 mg) at 60 °C for 24 h. Reactions were monitored by NMR spectroscopy. Oxidation of p-anisyl alcohol and benzoin using MIL-100(V) was performed under identical conditions and monitored with TLC and NMR.

3 Results and discussion

3.1 Overview of Synthetic Strategies

This study investigated several synthetic routes toward vanadium-containing MIL-100 materials, with the aim of replacing the previously reported VCl_3-based approach by more accessible and potentially greener vanadium precursors. The results show a clear distinction between direct synthesis attempts and incorporation by doping.

Direct hydrothermal and solvothermal routes using vanadium precursors such as $VOSO_4 \cdot 5H_2O$ and $V(acac)_3$ generally produced materials of low crystallinity or predominantly amorphous character, whereas synthesis of bimetallic MIL-100(Fe) and MIL-100(Al) frameworks with vanadium was more successful in preserving the characteristic MIL-100 topology. These findings indicate that the formation of a structurally well-defined vanadium-based MIL-100 framework is highly sensitive to the speciation and coordination behaviour of the vanadium precursor, as well as to the synthesis environment.

The synthesized MIL-100 materials were analysed using PXRD, FTIR, and TGA to confirm their structural and chemical characteristics. PXRD was used to determine whether the characteristic MIL-100 framework had formed and to assess the crystallinity and phase purity of the products, while FTIR confirmed the presence of the organic linker and metal-ligand coordination. TGA was used to evaluate thermal stability and guest content, and XRF was used to determine elemental composition in the bimetallic systems.

3.2 Hydrothermal and solvothermal syntheses

3.2.1 Initial synthesis attempts using $VOSO_4 \cdot 5H_2O$

Initial attempts to replace VCl_3 focused on using $VOSO_4 \cdot 5H_2O$ under solvothermal conditions. Synthesis was performed in DMF and water separately at 130 °C for 24 h, with triethylamine added to assist in deprotonation of the BTC acid linker. The results from these direct synthesis routes generally showed poor crystallinity. The PXRD patterns exhibited broad, ill-defined peaks or largely amorphous profiles, as shown in

Figure 3, suggesting that the MIL-100(V) framework did not fully form under these conditions. The low crystallinity observed in the direct synthesis attempts can be attributed to several issues related to the chemical behaviour of the vanadium source. $VOSO_4 \cdot 5H_2O$ contains the vanadyl cation, which is likely resistant to the hydrolysis and ligand substitution steps needed for MOF assembly under the conditions used.[39]

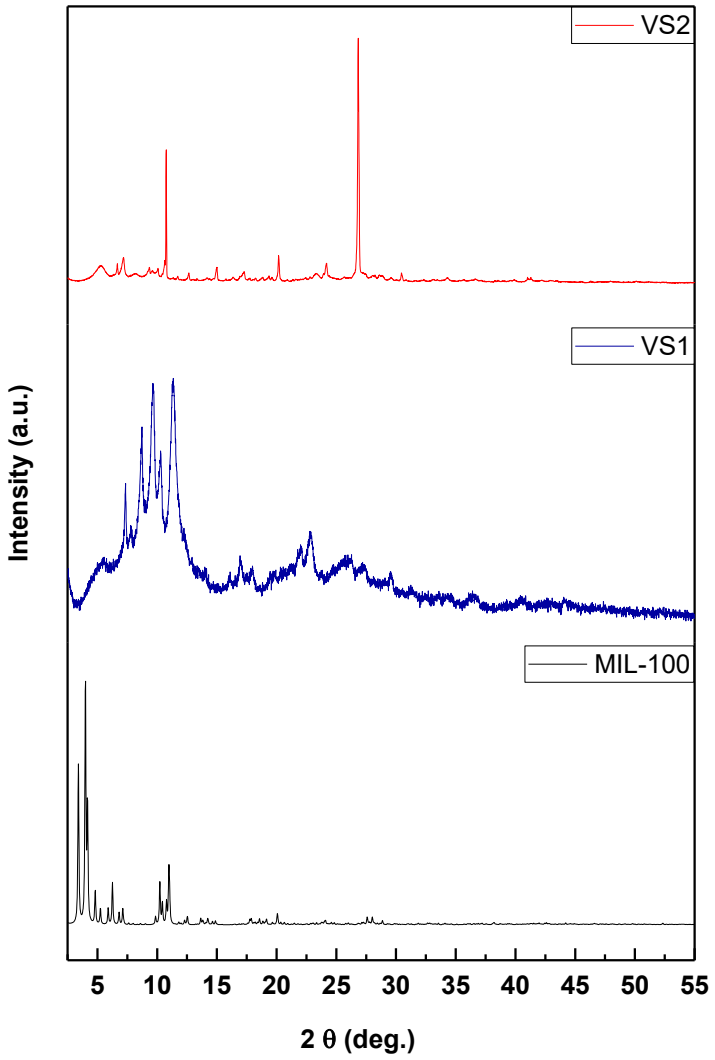

Figure 3 PXRD patterns of hydrothermal and solvothermal syntheses. Black: Published MIL-100(Fe) pattern adapted from Horcajada et al.[13] Blue: pattern for VS1 synthesized solvothermally from $VOSO_4 \cdot 5H_2O$ in DMF at 120 ºC. Red: VS2 synthesized hydrothermally from $VOSO_4 \cdot 5H_2O$ at 120 ºC.

In addition, the VO^{2+} cation typically adopts a square pyramidal shape, whereas the trimeric clusters required for MIL-100 formation require a different local coordination

environment.[19] For successful framework assembly, this vanadyl cation would need to undergo substantial speciation change and ligand exchange to support cluster formation. The mild hydrothermal and solvothermal conditions used here, ranging from 120 to 150 ºC for 24 to 48 h, could not overcome these thermodynamic and kinetic barriers. As a result, the products remained disordered or phase mixed rather than forming a well-defined crystalline MIL-100(V) structure.[41]

3.2.2 Synthesis with $V(acac)_3$

The use of $V(acac)_3$ provides a coordinatively saturated vanadium precursor with a different ligand environment but introduces a different set of challenges. The acetylacetonate ligands are strongly coordinating and must be displaced by the BTC acid linker during synthesis. Incomplete ligand exchange can result in the formation of defective frameworks in which some vanadium centres remain coordinated by acetylacetonate rather than BTC acid, disrupting the long-range order and reducing crystallinity.[42] Moreover, the acetylacetonate ligands can act as competing modulators, slowing the rate of framework assembly and potentially favouring the formation of kinetically trapped, poorly crystalline phases.[43]

The experimental PXRD pattern of the $V(acac)_3$-based synthesis did not reproduce the characteristic low-angle reflections reported for MIL-100(V). Instead, it shows features consistent with residual precursor-derived material and/or poorly crystalline vanadium phases. This suggests that, under the applied conditions, ligand exchange and framework assembly were incomplete, likely due to suboptimal control of pH, water content, and reaction temperature or time. The observed PXRD pattern of the $V(acac)_3$-based syntheses is shown in Figure 4 below.

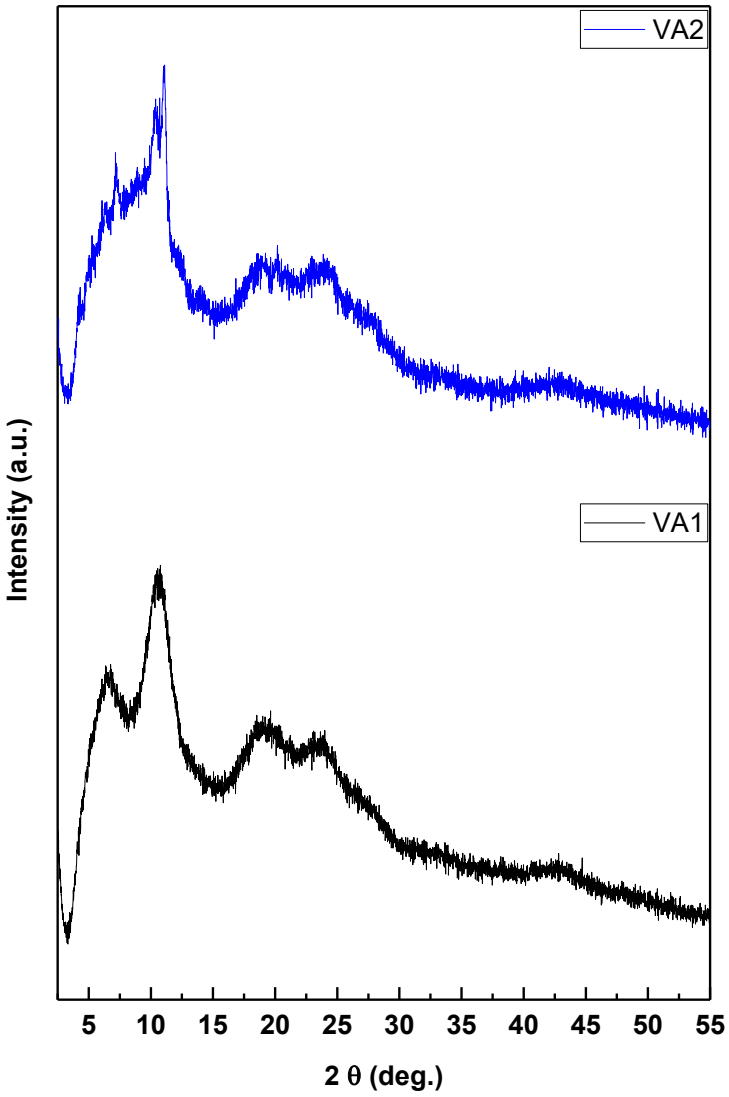

Figure 4 **PXRD patterns of $V(acac)_3$ syntheses.** Black: hydrothermal method. Blue: reflux method using DMF as the solvent.

3.2.3 Influence of solvent system on MIL-100(V) formation

The solvent system plays a critical role in controlling the solubility of the metal precursor and the organic linker, the rate of metal-ligand bond formation, and the dielectric environment that influences the stability of charged intermediates.[44] The PXRD patterns of the $VOSO_4 \cdot 5H_2O$ based syntheses in DMF:EtOH:H_2O, EtOH:H_2O, and H_2O did not reproduce the characteristic low angle reflections of MIL 100(V) reported in literature. Instead, the diffractograms exhibit broadened peaks and additional

reflections, indicative of poorly crystalline or mixed vanadium oxo/sulphate phases as seen on Figure 5.

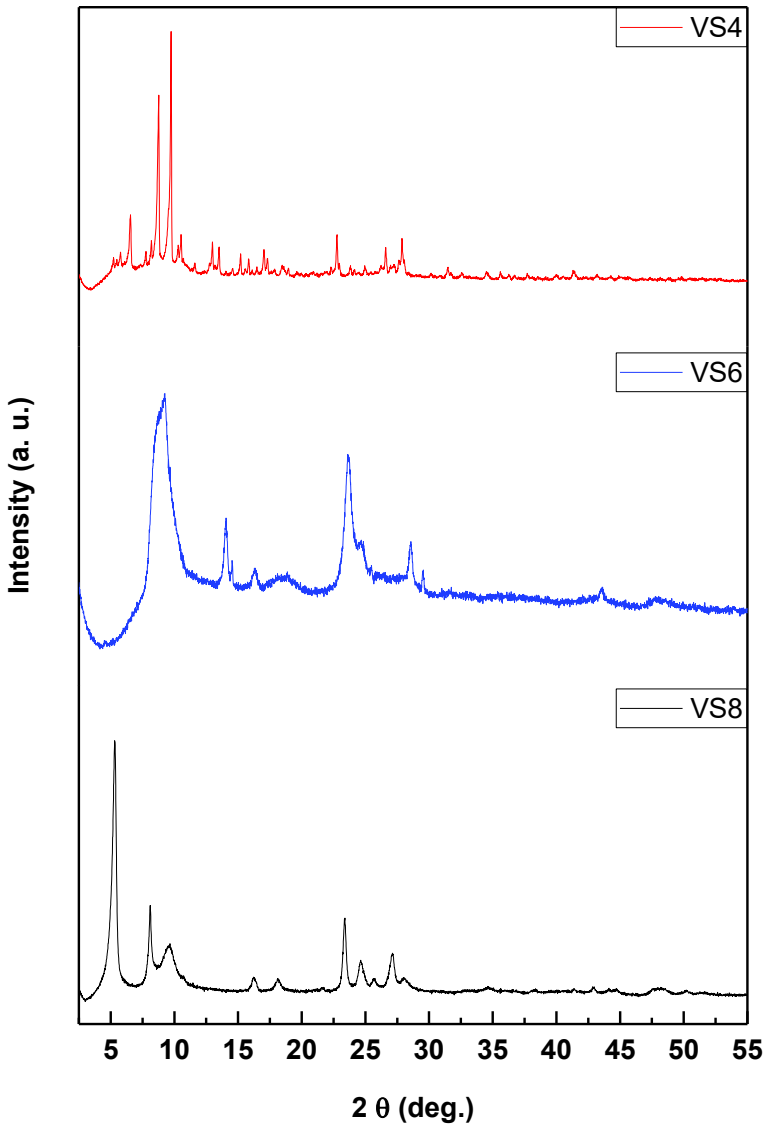

Figure 5 PXRD patterns comparing the effect of solvent systems at pH 2. VS4: synthesized from $VOSO_4 \cdot 5H_2O$ in DMF:EtOH:H_2O ratio (3:1:1). VS6: synthesized from $VOSO_4 \cdot 5H_2O$ in EtOH:H_2O (1:1). VS8: synthesized hydrothermally from $VOSO_4 \cdot 5H_2O$.

Solvothermal synthesis conducted in the DMF-containing mixture yielded materials with slightly higher crystallinity compared to purely aqueous hydrothermal synthesis, as evidenced by sharper PXRD peaks and higher peak intensities. This improvement can be attributed to the slower hydrolysis kinetics of vanadium precursors in DMF, which

allows for more controlled nucleation and crystal growth.[45] DMF may also stabilize intermediate vanadium-oxo species and prevent premature precipitation of amorphous phases.[46] However, even in DMF-based systems, the patterns remained significantly different from the literature patterns of MIL-100(V), indicating that solvent effects alone were insufficient to overcome the intrinsic challenges associated with MIL-100(V) synthesis.

3.2.4 Effect of pH and temperature

The synthesis temperature influences both the kinetics of framework assembly and the thermodynamic stability of the MOF phase relative to competing vanadium oxide phases. Higher temperatures (>200 °C) promote faster crystal growth and can improve crystallinity by providing sufficient thermal energy to overcome kinetic barriers to framework assembly.[47] However, elevated temperatures also increase the rate of oxide formation, particularly in the presence of water, and can lead to the decomposition of the MOF framework or the oxidation of V^{3+} to V^{4+} or V^{5+}.

In this study, synthesis temperatures of 130 –150 °C were used for most experiments, which are typical for solvothermal MOF synthesis but may be insufficient to promote the formation of highly crystalline MIL-100(V). Attempts to increase the temperature to 240 °C in the presence of HCl resulted in the formation of vanadium oxide phases rather than the MIL-100 topology, confirming that a delicate balance between kinetic and thermodynamic factors must be achieved to obtain phase-pure MIL-100(V).

The pH of the synthesis medium influences the hydrolysis and condensation behaviour of vanadium species the deprotonation state of the linker. The formation of the MIL-100 topology requires the assembly of trimeric vanadium-oxo clusters coordinated by carboxylate groups from the BTC acid linker.[19] Such clusters are generally favoured under acidic conditions, where vanadium hydrolysis is moderated, but excessively low pH can protonate the linker and hinder coordination.[48] Conversely, at higher pH (pH > 4), vanadium undergoes extensive hydrolysis and condensation, forming large, insoluble vanadium hydroxide or oxide aggregates that are incompatible with MOF formation. The PXRD patterns obtained through synthesis at low pH values and different temperatures is shown in Figure 6.

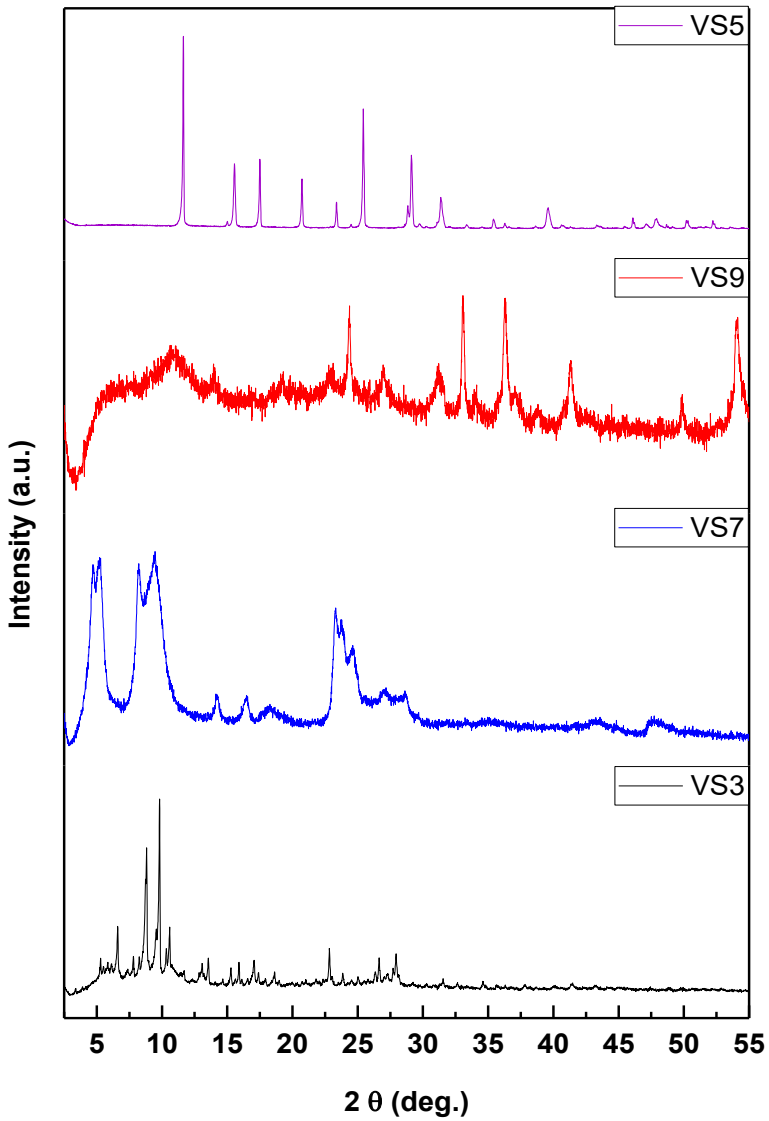

Figure 6 PXRD patterns comparing the effect of temperature and pH. VS3: synthesized from $VOSO_4 \cdot 5H_2O$ in DMF:EtOH:H_2O (3:1:1) at 120 ºC and pH 2. VS7: synthesized from $VOSO_4 \cdot 5H_2O$ EtOH:H_2O (1:1) at 120 ºC and pH 2. VS7: synthesized hydrothermally from $VOSO_4 \cdot 5H_2O$ 120 ºC and pH 2. VS9: synthesized from $VOSO_4 \cdot 5H_2O$ in DMF:EtOH:H_2O (3:1:1) with HCl at 240 ºC.

Syntheses were conducted at pH values ranging from 0.5 to 2, which are within the optimal range for MIL-100(Fe) and MIL-100(Al) synthesis.[18,34] However, the low crystallinity observed in the vanadium-based syntheses suggests that the pH window for MIL-100(V) formation may be narrower or shifted relative to that of the Fe and Al analogues. Fine-tuning the pH through the addition of controlled amounts of acid, for

example HCl or HNO_3, or base, for example NaOH or triethylamine, may be necessary to identify the optimal conditions for MIL-100(V) crystallization.

Synthesis in the presence of HF

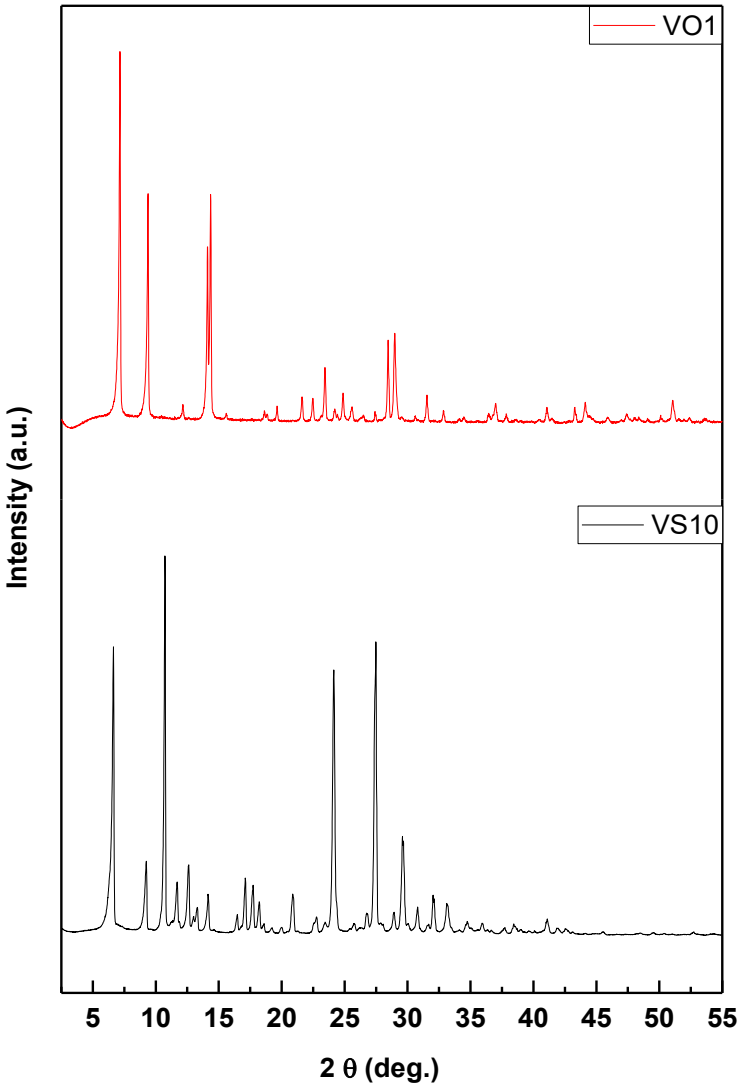

Figure 7 PXRD patterns of HF-mediated. Black: product from $VOSO_4.5H_2O$. Red: product from V_2O_5. Both samples show crystalline phases that do not match the MIL-100 topology.

The PXRD patterns of the products obtained using HF-mediated synthesis in Figure 7 do not show the characteristic low-angle reflections expected for the MIL-100 topology, indicating that the long-range mesoporous framework failed to form. Instead, the observed diffractograms show a set of reflections that differ significantly from the

reported MIL-100 fingerprint, suggesting the formation of alternative crystalline vanadium-containing phases or disordered solids. While fluoride ions are typically effective mineralizing agents for stabilizing trimeric clusters in MIL-100(Fe) and MIL-100(Cr) synthesis,[10] these results indicate that they are insufficient to direct the assembly of vanadium species into the MIL-100 architecture under the current conditions. The lack of characteristic mesoporous-related reflections confirms that competing vanadium oxide or precursor-derived phases are thermodynamically and kinetically favoured, demonstrating that the synthesis of phase-pure MIL-100(V) remains a significant challenge that cannot be overcome by HF-assisted mineralisation alone.

3.3 Bimetallic synthesis and post-synthetic incorporation

Given the challenges encountered with direct crystallization from vanadium precursors, alternative strategies for obtaining vanadium-containing MIL-100 materials were explored. In contrast to the challenges encountered in the direct synthesis of MIL-100(V), the bimetallic synthesis approaches proved to be significantly more successful. The PXRD patterns of vanadium containing MIL-100(Fe) and vanadium-containing MIL-100(Al) exhibited features consistent with the characteristic MIL-100 topology, although the degree of crystallinity varied between the two systems The preservation of the MIL-100 structure upon vanadium incorporation indicates that the introduction of vanadium process does not destroy the framework architecture and that vanadium is incorporated either by substitution in the trimeric clusters or by occupation of defect-related sites.

3.3.1 Bimetallic MIL-100(Fe,V)

Bimetallic MIL-100(Fe,V) materials with varying Fe:V ratios were synthesized to investigate the incorporation of vanadium into the MIL-100(Fe) framework. The PXRD patterns of these frameworks were notably broad and of low intensity, indicating that the materials retained only partial structural order.

Several factors may contribute to this disorder. Partial substitution of Fe by vanadium species can introduce heterogeneity in the trimeric metal-oxo clusters, with some

clusters containing only Fe, others only vanadium, and others mixed Fe-V compositions. This compositional heterogeneity can disrupt the periodicity of the framework and reduce crystalline coherence.[49] Differences in preferred coordination geometry and bond lengths between Fe and vanadium may also introduce local lattice distortions that broaden PXRD peaks. Additionally, the rapid nucleation of the MIL-100(Fe) framework under the synthesis conditions employed may favour the formation of small, disordered particles rather than highly crystalline materials, and the subsequent incorporation of vanadium may not be sufficient to anneal these defects.[50]

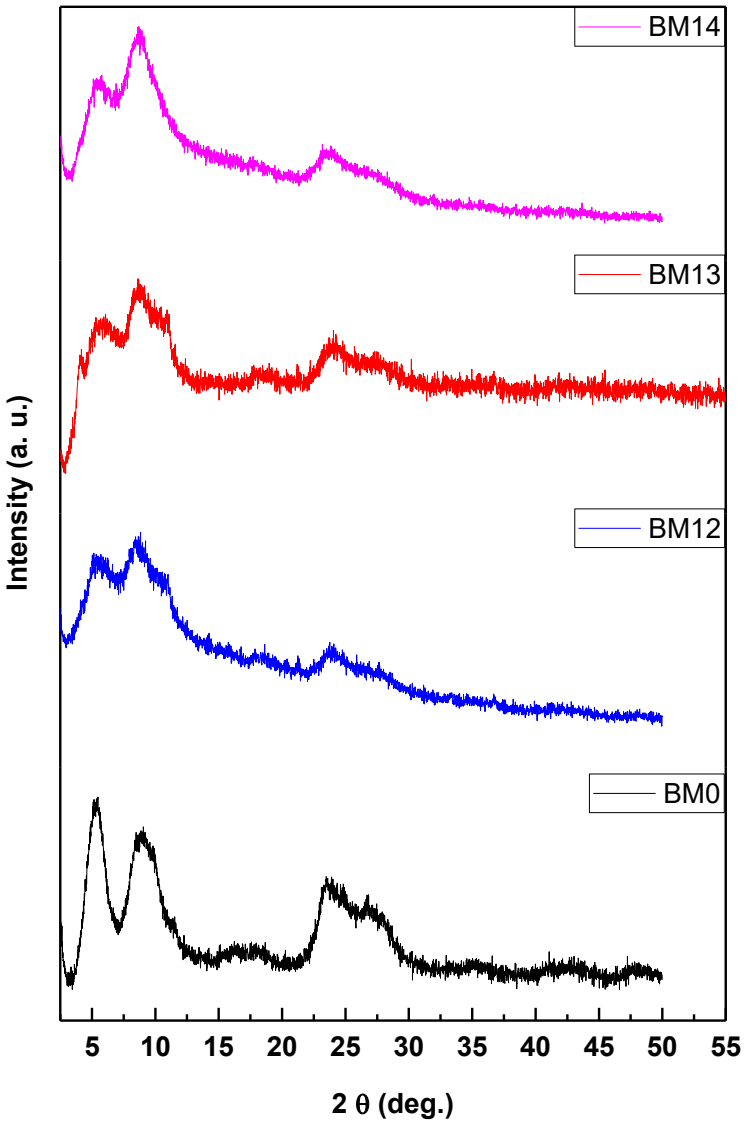

Figure 8 PXRD patterns of bimetallic MIL-100(Fe,V) samples. BM0: synthesized from $VOSO_4 \cdot 5H_2O$ only. BM12: synthesized with an Fe:V ratio of 1:2. BM13: synthesized with an Fe:V ratio of 1:3. BM14: synthesized with an Fe:V ration of 1:4.

Despite the low crystallinity, the presence of low-angle reflections suggests that some MIL-100-type ordering is retained. These results indicate that the bimetallic synthesis strategy is effective for introducing vanadium into MIL-100(Fe), but further optimisation of synthesis conditions would be required to improve crystallinity and structural definition.

The procedure was also extended to the synthesis of a vanadium-containing MIL-100 phase without iron. This reaction was conducted at room temperature in water with NaOH and BTC acid for 24 h. The resulting material exhibited a PXRD pattern consistent with the MIL-100 topology, confirming that a vanadium-containing MIL-100 phase can be formed without VCl_3. However, the crystallinity remained relatively low as observed in the PXRD pattern in Figure 8 above.

This room-temperature approach represents a significant advancement in green MOF synthesis, eliminating the need for energy-intensive heating and specialized autoclave equipment. The method is consistent with recent reports of green, scalable synthesis of bimetallic MIL-100(Fe,M) materials at room temperature in aqueous media.[5] Steenhaut et al. showed that this method can be used to incorporate p-, d-, and f-block elements in oxidation states ranging from +1 to +5. The incorporation of vanadium into the MIL-100(Fe) framework at room temperature suggests facile metal exchange or co-assembly processes that do not require elevated temperatures.[51]

3.3.2 Bimetallic MIL-100(Al,V)

The most successful route for obtaining crystalline vanadium-containing MIL-100 was the addition of vanadium into a MIL-100(Al) framework. The PXRD patterns of bimetallic MIL-100(Al,V) showed sharp, high-intensity peaks that closely matched those of the pure MIL-100(Al) phase, indicating that the structural integrity of the framework is perfectly maintained upon vanadium incorporation. This result suggests that vanadium is likely incorporated into or near aluminium-containing trimeric sites or occupying coordinatively unsaturated sites within the framework without disrupting the long-range order of the crystal. The high crystallinity of the bimetallic MIL-100(Al,V) materials is particularly noteworthy given the low crystallinity observed in the direct synthesis attempts, and it highlights the utility of post-synthetic addition as a strategy for introducing vanadium into MIL-100 frameworks while preserving structural quality. The crystallinity in the PXRD patterns obtained for the MIL-100(Al) and BMAl are shown in Figure 9.

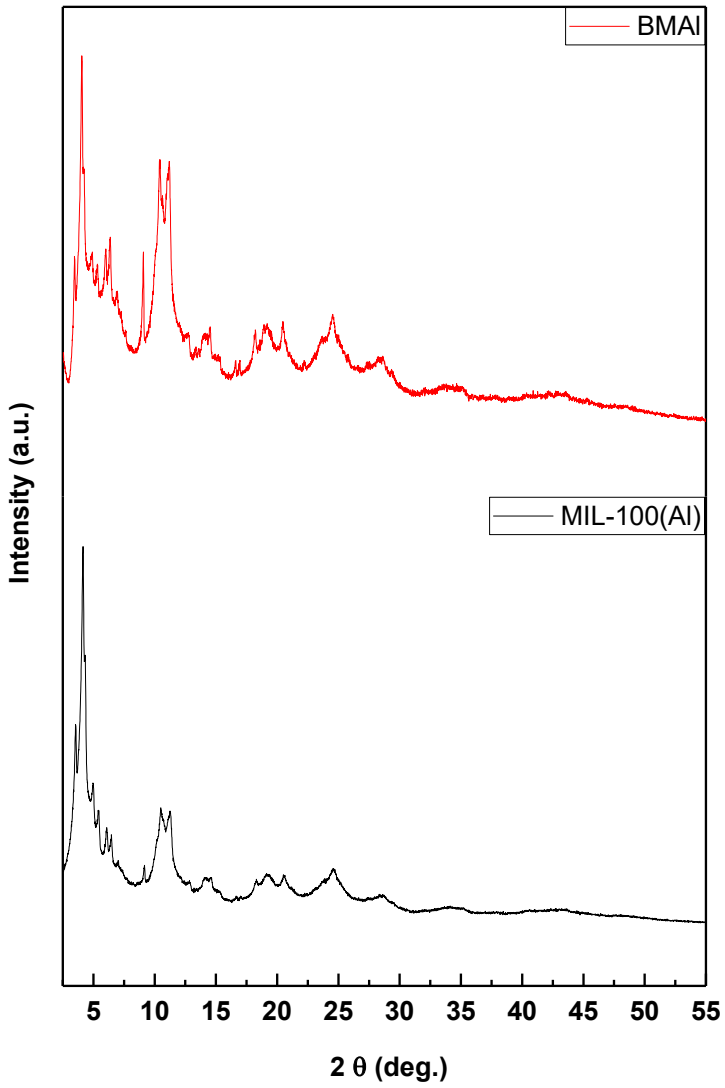

Figure 9 PXRD patterns of MIL-100(Al) and vanadium-incorporated MIL-100(Al). Black: MIL-100(Al). Red: BMAl.

The success of the bimetallic synthesis approach can be explained in terms of the thermodynamic and kinetic factors that govern framework assembly. In the direct synthesis of MIL-100(V), the formation of the trimeric vanadium-oxo cluster and its assembly into the extended framework must occur simultaneously, and any kinetic or thermodynamic barriers to cluster formation or framework assembly will result in low crystallinity or the formation of competing phases.[52] In the bimetallic synthesis approach, the MIL-100(Al) framework is pre-formed and provides a crystalline template

into which vanadium can be introduced. This pre-existing framework constrains the local coordination environment of the vanadium centres and suppresses the formation of alternative vanadium-containing phases.[6]

3.4 Elemental composition by XRF

XRF is a non-destructive method used to identify the elemental makeup of a material. It operates by exposing a sample to primary X-rays, which knock out inner-shell electrons from the atoms. As electrons from higher energy levels move down to fill these gaps, they release secondary X-rays that are characteristic of specific elements. XRF can therefore be used for both qualitative identification and quantitative compositional analysis. XRF is particularly valuable because it can confirm whether a target metal has been incorporated into a sample and can estimate the relative abundance of different metal species.[53]

In this study, XRF was especially important for verifying vanadium incorporation into the MIL-100 samples and for comparing the measured metal ratios with the intended synthesis ratios. This was necessary because PXRD can show whether a framework structure is present, but it does not directly quantify elemental composition. XRF therefore complements PXRD by showing whether vanadium was successfully introduced into the material, whether iron or aluminium remained present in the doped systems, and whether the experimental ratios matched the designed compositions. For the bimetallic MIL-100(Fe,V) and MIL-100(Al,V) samples, XRF helps distinguish true metal incorporation from simple physical mixing or surface contamination. The Fe and V compositions of the bimetallic MIL-100(Fe) samples are shown in Table 2.

BM0 was found to be composed of 98.5% V, indicating a very high vanadium content. Its iron content was only 225 ppm, which is consistent with trace contamination from the starting materials, handling, or the synthesis environment. Other detected elements included silicon, sulphur, and chlorine, which are likely associated with minor impurities, precursor residues, or environmental contamination rather than the core framework structure.

Table 2 XRF values obtained for the different bimetallic MIL-100(Fe,V) variants

Product	Amount of Fe (%)	Amount of V (%)
BM12	45.7	49.5
BM13	42.5	53.8
BM14	18.6	76.9
BM0	< 1.00	98.5

For BMAl, XRF showed 39.8% vanadium content and an aluminium content of 46.7%, indicating substantial incorporation of vanadium while still retaining a large aluminium fraction. The bimetallic synthesis process likely involves partial replacement of Fe^{3+} or Al^{3+} ions in the trimeric metal-oxo clusters by vanadium species from solution, or incorporation of vanadium into defect sites or near-surface positions.

The bimetallic synthesis process likely involves partial replacement of Fe^{3+} or Al^{3+} ions in the trimeric metal-oxo clusters by vanadium species from solution, or incorporation of vanadium into defect sites or near-surface positions. In MIL-100(Al, Fe), the metal trimers are known to contain mixed-metal clusters with randomly distributed trivalent ions, showing that substitution among trivalent metals can occur within the framework. The structural compatibility of Fe^{3+}, Al^{3+}, and V^{3+} also supports this interpretation, since these ions have similar octahedral coordination preferences and comparable ionic radii in six-coordinate environments. Because of this similarity, vanadium can be introduced without necessarily causing complete structural collapse.

The fact that BMAl exhibited higher crystallinity than BM21 and other MIL-100(Fe,V) variants may reflect differences between in-situ synthesis and post-synthetic metal exchange. In practical terms, this means that XRF confirms vanadium uptake in both systems, but the degree of uptake should not be interpreted as proof of complete or uniform metal substitution across the framework.

3.5 Fourier Transform Infrared Spectroscopy

FTIR analysis provides an important complement to PXRD because it verifies the presence of the organic linker and offers indirect evidence for metal–ligand coordination within the framework. In MIL-100-type materials, the most informative spectral region is

the carboxylate stretching range, where coordination to metal nodes alters the vibrational environment of the linker relative to the free acid. The spectrum obtained for BM0 in Figure 11 shows the expected bands associated with the benzene-1,3,5-tricarboxylate framework, including strong absorptions in the fingerprint region and bands in the carboxylate region, indicating that the organic linker remains present after synthesis. This supports the conclusion that at least local metal–ligand coordination has occurred, even if the material is not fully crystalline by PXRD.

The broad feature in the high-wavenumber region, roughly between 3600 and 3000 cm^{-1}, can be assigned to O-H stretching vibrations from adsorbed water and residual solvent retained in the pores of the material. Such broad O-H bands are common in porous MOFs, especially in samples that have not been fully activated or that retain coordinated or physisorbed water. In a vanadium-containing MOF, this feature may also reflect hydroxyl groups associated with partially hydrolysed metal species or with incomplete condensation during framework formation. The presence of this band therefore suggests that the sample still contains guest molecules or hydroxylated species, which is consistent with a material that has not yet reached complete pore evacuation or structural perfection.[54]

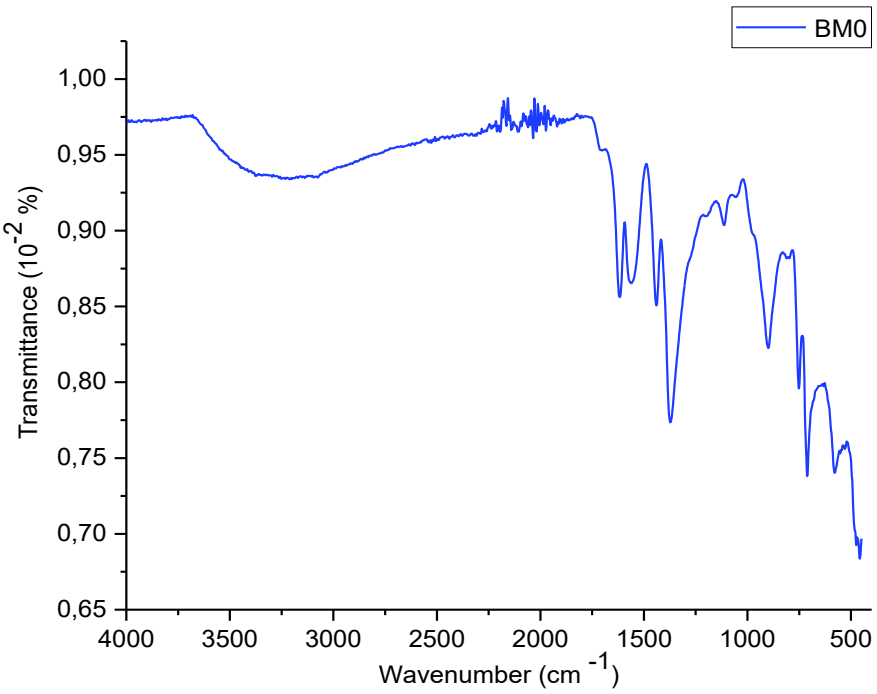

Figure 10 FTIR spectrum of BM0. The spectrum shows broad O–H stretching bands in the high-wavenumber region and carboxylate stretching vibrations in the 1600–1400 cm^{-1} region.

In the carboxylate region, the bands around 1600–1400 cm^{-1} are particularly important because they are associated with asymmetric and symmetric stretching of coordinated carboxylate groups. In MIL-100 materials, these bands are expected to shift relative to the free BTC acid precursor, reflecting deprotonation of the linker and coordination to the metal centres. The presence of these bands in the BM0 sample indicates that the linker is not merely physically adsorbed but is chemically bound within a metal-organic environment. This is significant because it shows that the reaction did not simply yield a mixture of precursors, but instead produced at least partial framework assembly.[55]

Overall, the FTIR spectrum supports the interpretation that the BM0 sample contains coordinated BTC acid linkers and retained framework-associated species. When considered together with the PXRD results, the FTIR data suggest that the synthesis produced a chemically valid but only partially ordered MIL-100-type material. This is consistent with the broader result of the study, namely that vanadium-containing MIL-100 phases could be obtained, but their crystallinity and phase purity depended strongly on the synthesis route.

3.6 Thermogravimetric Analysis

TGA provides information on the thermal stability, guest content, and decomposition behaviour of the MIL-100 samples. In porous MOFs, the earliest mass-loss event is usually assigned to removal of physically adsorbed water, trapped solvent molecules, or other weakly bound guest species from the pores, while the major mass-loss step at higher temperature corresponds to degradation of the organic linker and collapse of the framework. For vanadium-containing MIL-100 materials, this makes TGA especially useful for judging whether the synthesized solids contain substantial amounts of occluded solvent or water and whether the framework is stable enough to withstand activation and subsequent catalytic use.

The TGA profile obtained for the BM0 sample indicates an initial gradual weight loss below about 150 ºC, followed by a slower decline up to approximately 350 ºC. This first region is consistent with the release of adsorbed water and residual solvent molecules. The relatively modest slope in this region suggests that the sample contains some guest species, but not an exceptionally large amount compared with a heavily solvated or highly defective MOF. This is in line with the FTIR spectrum, which also showed broad O–H absorption associated with retained water or hydroxylated species.

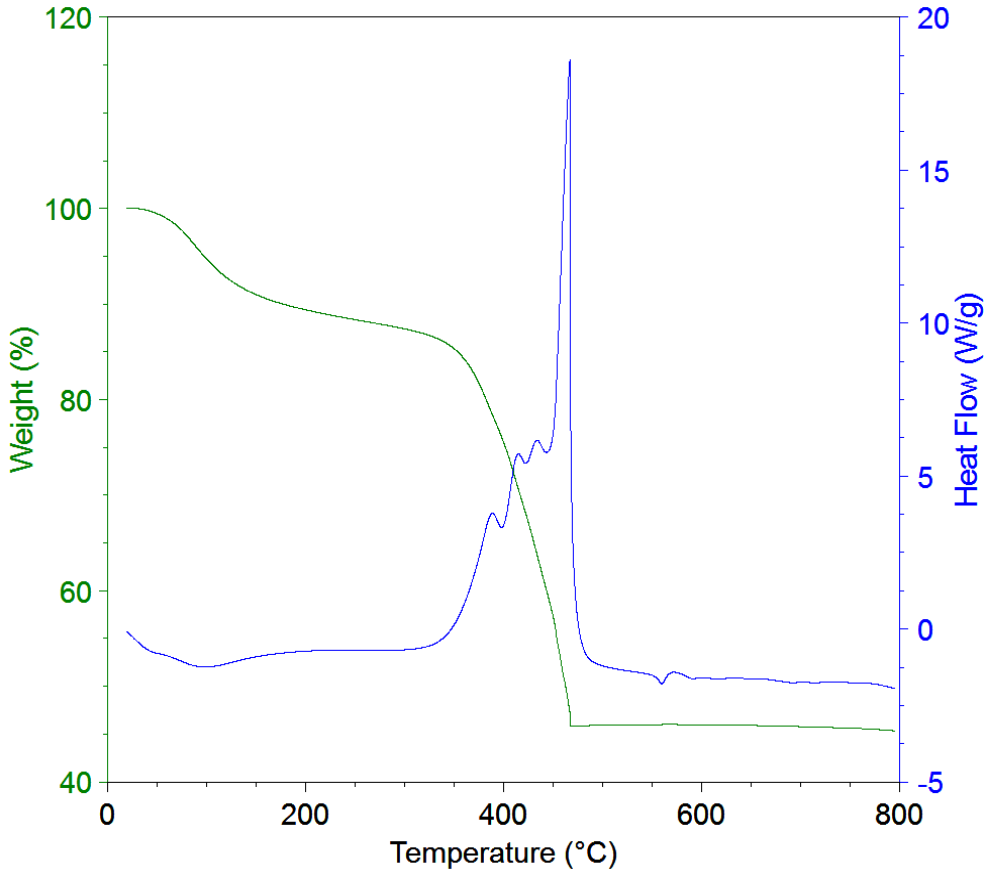

Figure 11 TGA curve for BM0. The sample is stable up to approximately 350 °C, followed by major framework decomposition at higher temperature.

A more pronounced mass-loss event begins around 350–450 ºC, where the curve drops steeply and the heat-flow signal shows a strong transition. This step is best assigned to decomposition of the BTC acid linker and breakdown of the MIL-100 framework. The sharpness of this transition suggests that a chemically distinct framework component is present and undergoes a major decomposition event over a relatively narrow temperature range, which supports the presence of an ordered MOF-like structure rather than a completely amorphous residue. At the same time, the fact that decomposition begins before 500 ºC indicates that the framework is stable up to several hundred degrees, which is typical for many MIL-100-type materials.

After the major decomposition step, the mass becomes nearly constant at about 45-46 % residue above roughly 500 ºC. This remaining mass is consistent with an inorganic residue, likely containing vanadium oxides. For a vanadium-rich framework, a relatively high final residue is expected because the metal content contributes substantially to

the remaining mass after thermal decomposition. The plateau also suggests that most volatile and organic components have been removed by this point, leaving a thermally stable inorganic residue.

Overall, the TGA result supports the interpretation that the sample contains a porous vanadium-based MIL-100 material with retained guest species, moderate thermal stability, and a well-defined decomposition step associated with framework collapse. In combination with the FTIR and PXRD data, the TGA profile suggests that the synthesized sample is chemically consistent with a MIL-100-type material, even though the crystallinity is not fully ideal.

4 Applications of MIL-100(V) in heterogeneous catalysis

4.1 Catalytic addition of CO_2 to epoxide

The catalytic cycloaddition of CO_2 to styrene oxide is a useful test reaction for evaluating whether a MOF can function as a heterogeneous Lewis acid catalyst. In an ideal system, the epoxide is first activated by coordination to an accessible metal site, after which a nucleophilic co-catalyst promotes ring opening and enables insertion of CO_2 to form the cyclic carbonate. The absence of detectable conversion in this study therefore suggests that the vanadium-containing MIL-100 materials did not provide a sufficiently effective combination of Lewis acidity, accessible pore environment, and cooperative activation sites under the reaction conditions employed.

This result is not unexpected for a partially crystalline or defect-rich MOF. CO_2 cycloaddition usually requires a catalyst with open metal centres that are both accessible and stable, as well as a suitable nucleophile such as a halide salt to assist epoxide ring opening. If the framework contains residual solvent, blocked pores, or only a low density of exposed active sites, substrate diffusion into the material and coordination to the metal centres may be strongly limited. In that case, the catalytic cycle cannot proceed efficiently even if vanadium is present in the framework.

The lack of conversion may also reflect the intrinsic difficulty of promoting CO_2 cycloaddition under mild conditions. Even when MOFs are active in this transformation, performance is often improved by higher CO_2 pressure, elevated temperature, longer reaction time, or a more effective co-catalyst system. Under the relatively mild conditions used here, the system may not have been forceful enough to overcome the energetic barrier for epoxide ring opening. The single TLC spot corresponding to styrene oxide throughout the reaction therefore indicates that the material was either catalytically inactive for this transformation or only weakly active below the detection limit of the method.

4.2 Oxidation reactions

The oxidation studies were designed to assess whether the vanadium-containing MIL-100 materials could function as heterogeneous redox catalysts after activation. Vanadium-based MOFs are attractive for oxidation chemistry because vanadium can access multiple oxidation states and can promote oxygen-transfer reactions through coordinatively unsaturated sites or surface-bound oxo species. However, catalytic performance in such systems depends not only on the presence of vanadium, but also on framework crystallinity, site accessibility, guest removal during activation, and the ability of the substrate to diffuse into the pores. The substrate-dependent outcomes observed in this study are therefore consistent with the broader MOF literature, where activity often varies strongly with substrate size, oxidant efficiency, and the stability of the catalyst under reaction conditions.[19,56,57]

The study used three primary catalysts: BM0, BM12, and BMAl. Each MOF underwent an activation process involving chloroform washing followed by drying under vacuum to remove guest molecules and generate coordinatively unsaturated metal sites. These open metal sites act as Lewis acid centres, facilitating the activation of tert-BuOOH. The catalysts were tested on cis-cyclooctene, thioanisole, benzyl alcohol, p-anisyl alcohol, and benzoin at 60 ºC for 24 h.

4.2.1 Oxidation of cis-cyclooctene

The oxidation of cis-cyclooctene is a useful probe reaction because the substrate is relatively accessible and epoxidation is often used to evaluate the presence of redox-active metal sites in porous catalysts. In vanadium-containing MOFs, epoxidation can proceed through formation of a reactive metal-oxo or peroxide intermediate that transfers an oxygen atom to the alkene. If the catalyst surface is sufficiently active and the pores remain accessible after activation, the reaction can provide a quick measure of whether the vanadium sites are redox competent.[56,58]

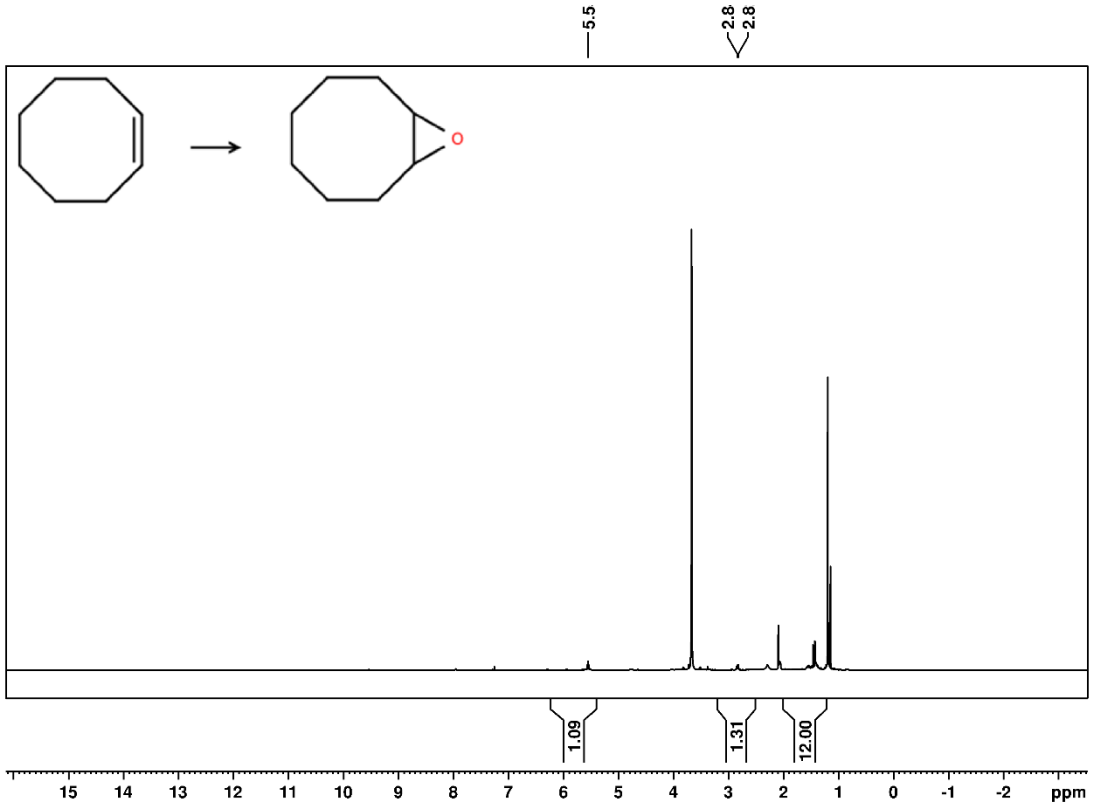

Figure 12 NMR spectrum of the catalytic oxidation of cis-cyclooctene showing resonances for both the product epoxide oxygen and the unreacted cis-cyclooctene.

The obtained ^{1}H NMR spectrum in Figure 12 shows that the reaction mixture contains a mixture of both the starting alkene and the epoxide product of cis-cyclooctene oxidation. The signal at about 5.5 ppm can be assigned to the olefinic protons of unreacted cis-cyclooctene, while the new resonances around 2.8–3.2 ppm are consistent with protons adjacent to the epoxide oxygen in cyclooctene oxide. The observed conversion was limited, suggesting that the density of accessible vanadium sites was not high enough, or that the active species were only partially generated during the activation step. It is also possible that some vanadium sites were structurally embedded or blocked by residual solvent, which would reduce the number of catalytically available centres.[58]

The limited activity may also reflect the difference between structural vanadium incorporation and true catalytic site formation. In porous MOFs, oxidation performance is often improved when coordinatively unsaturated metal sites are generated by thermal or solvent activation, because those sites can bind oxidant and substrate more

effectively. If the material retained guest molecules or had only partial crystallinity, the epoxidation of cis-cyclooctene would be expected to remain modest even if vanadium was present in the bulk structure. The result therefore suggests that vanadium incorporation alone is not sufficient; the local site environment must also be open, stable, and accessible.[56,57,59]

4.2.2 Oxidation of thioanisole

Thioanisole oxidation is a classic test for selective sulphur oxidation because it can yield sulphoxide and, under stronger oxidation conditions, sulphone. Vanadium-based catalysts often perform well in sulphur oxidation because vanadium oxo species can transfer oxygen to sulphur efficiently while retaining a heterogeneous framework environment. In an ideal catalytic system, controlled oxidation would give predominantly sulphoxide at lower conversion and possibly sulphone under more vigorous conditions. The mixture of products observed in this study indicates that the catalyst promoted oxidation, but selectivity was not tightly controlled.[56,58]

The ^{1}H NMR spectrum in Figure 13 shows that oxidation of thioanisole by synthesized MIL-100(V) was incomplete, because the sample contains a mixture of unreacted thioanisole, methyl phenyl sulphoxide, and a smaller amount of methyl phenyl sulphone. This is evident from the methyl resonances: the starting sulphide methyl signal remains near 2.4–2.5 ppm, while new downfield singlets appear at about 2.7–2.8 ppm for the sulphoxide and around 3.0–3.1 ppm for the sulphone. The aromatic region remains consistent with a monosubstituted benzene ring, confirming that the phenyl group is retained throughout.

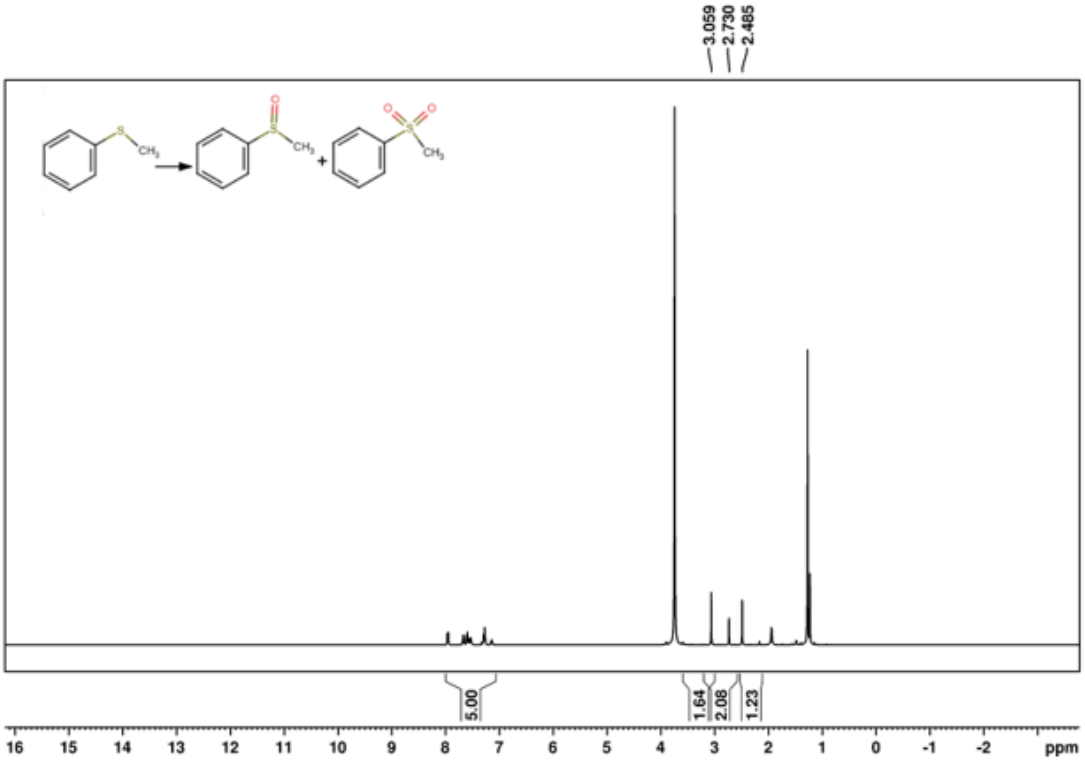

Figure 13 NMR spectrum of the oxidation of thioanisole. The spectrum shows that both the sulphoxide and sulphone are formed and the starting thioanisole is still present.

4.2.3 Oxidation of benzyl alcohol

Vanadium-MOF catalysts have been reported to promote selective oxidation of aromatic alcohols to aldehydes, and MIL-100(V) has specifically been shown to switch selectivity between benzaldehyde and benzoic acid depending on temperature and oxidant conditions. That makes benzyl alcohol a highly informative substrate for evaluating whether the synthesized MOFs can support controlled aerobic or peroxide-driven oxidation. In many systems, the alcohol first oxidizes to benzaldehyde, and further oxidation to benzoic acid can occur if the catalyst is sufficiently active or the reaction conditions are sufficiently promoting.[56,60]

The ^{1}H NMR spectrum obtained shows that MIL-100(V) catalysed the oxidation of benzyl alcohol to benzaldehyde, but the conversion was incomplete as seen in Figure 14 below. This is observed from the appearance of a new singlet at about 9.9 ppm, which shows the presence of the aldehyde proton in benzaldehyde, together with a remaining

signal around 4.6 ppm from the benzylic CH_2 group of unreacted benzyl alcohol. The aromatic signals in the 7–8 ppm region are consistent with a monosubstituted phenyl ring in both compounds, so the spectrum reflects a mixture of starting alcohol and aldehyde product rather than full oxidation.

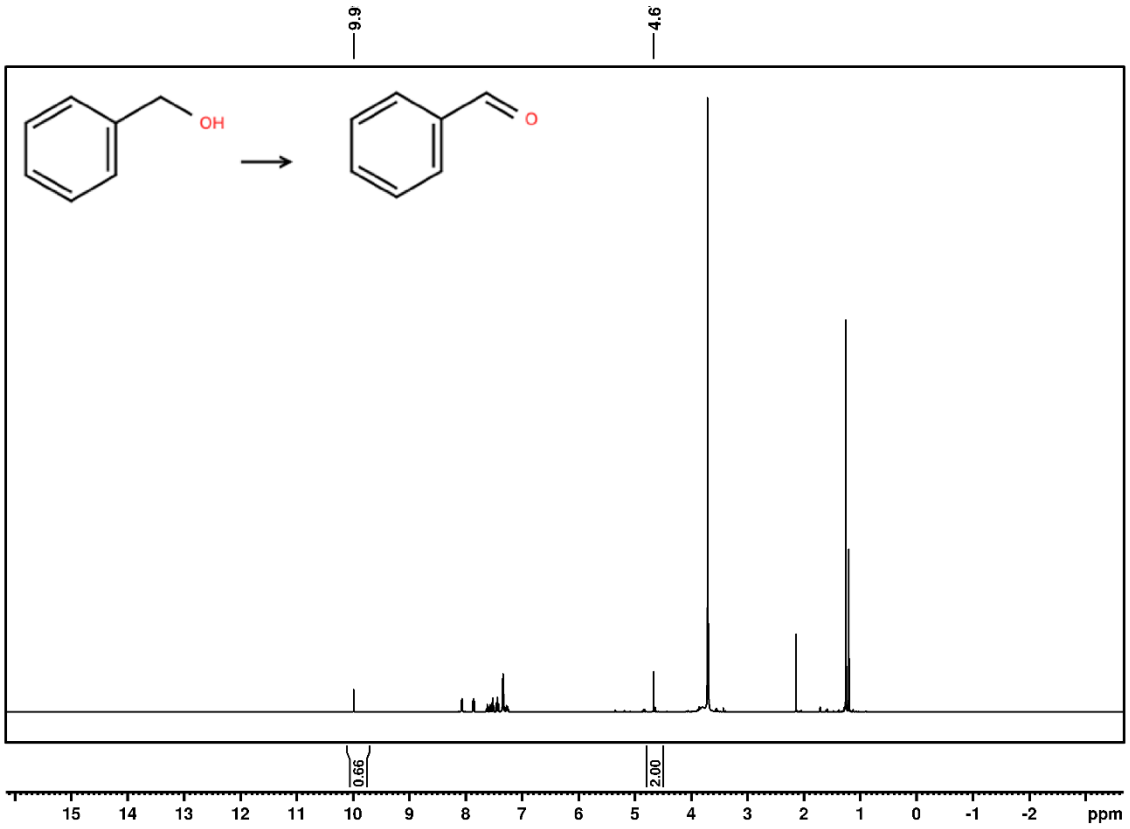

Figure 14 NMR spectrum for the oxidation of benzyl alcohol showing a new product proton peak at 9,9 ppm and the unreacted precursor protons at 4.6 ppm

The oxidation of benzyl alcohol was only partial, which suggests that the system could initiate oxidation but is not efficient enough to drive complete conversion under the applied conditions. This may be due to limited oxidant activation, low accessible vanadium site density, or insufficient contact between the substrate and the catalytic centres inside the porous framework. It is also possible that the reaction stopped at the aldehyde stage because the catalyst was not active enough for the second oxidation step, which is consistent with kinetic studies showing that benzyl alcohol oxidation and benzaldehyde oxidation can proceed at different rates even on the same catalyst. The experimental data therefore support the interpretation that benzyl alcohol is a suitable

probe for vanadium redox activity, but the present catalyst preparation did not yet provide a highly efficient oxidation system.

4.2.4 Oxidation of p-anisyl alcohol

In the oxidation of p-anisyl alcohol, the methoxy group changes the electronics of the aromatic ring, influencing the ease of alcohol oxidation. Electron-donating substituents often make benzylic oxidation more sensitive to catalyst redox behaviour and may alter the balance between alcohol-to-aldehyde conversion and overoxidation. For vanadium-based catalysts, the key question is whether the active sites can abstract hydrogen and deliver oxygen selectively without causing excessive side reactions.[56,61]

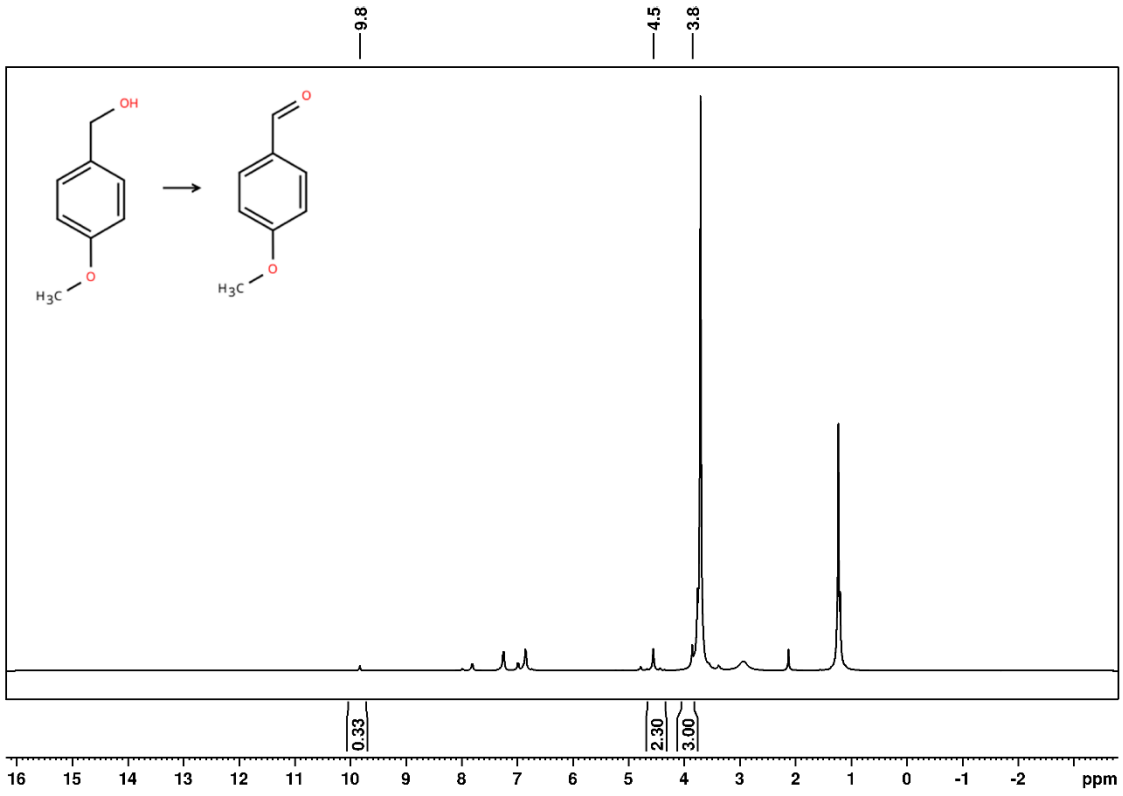

Figure 15 NMR spectrum for the catalytic oxidation of p-anisyl alcohol showing partial oxidation due to the presence of both the precursor peak at 4.5 ppm and the product peak at 9.8 ppm.

The ^{1}H NMR spectrum obtained in Figure 15 indicates that BM0 oxidized p-anisyl alcohol only partially to p-anisaldehyde. The appearance of a new singlet at about 9.8 ppm confirms the presence of the aldehyde proton in the product, confirming oxidation of the benzylic alcohol to an aldehyde, while signals in the 4.5–3.8 ppm region show that

unreacted p-anisyl alcohol is still present. The aromatic and methoxy resonances remain consistent with a para-methoxybenzyl framework, so the transformation is selective for oxidation at the benzylic position, but the relative integrals indicate incomplete conversion rather than full consumption of the starting alcohol.

The limited conversion is consistent with a catalyst that has accessible redox sites but possibly insufficient uniformity or pore accessibility. In MOF oxidation studies, aromatic alcohols often respond well only when the catalyst offers both open metal sites and sufficient mass transport through the pore system. The result also suggests that p-anisyl alcohol may be more demanding than benzyl alcohol under the same conditions, likely because subtle electronic effects and steric factors influence its reaction rate.[56–58]

4.2.5 The Exceptional Reactivity of Benzoin

In contrast to the other substrates, the oxidation of benzoin was uniquely successful, reaching full conversion to completion. Benzoin oxidation is an especially informative substrate because it converts to benzil through dehydrogenative oxidation, and this transformation is frequently used to evaluate the oxidative strength of heterogeneous catalysts.

The ^{1}H NMR spectrum obtained in Figure 16 indicates that benzoin was oxidized to benzil. The disappearance of the benzylic hydroxyl-bearing proton signal of benzoin at approximately 5.8–6.0 ppm supports conversion of the secondary alcohol to the corresponding diketone. The spectrum is dominated by aromatic resonances in the 7.3–8.0 ppm region, which are consistent with the two phenyl rings of benzil. This high level of conversion was further verified by TLC, which showed the absence of the benzoin spot and the formation of a single product spot corresponding to benzil.

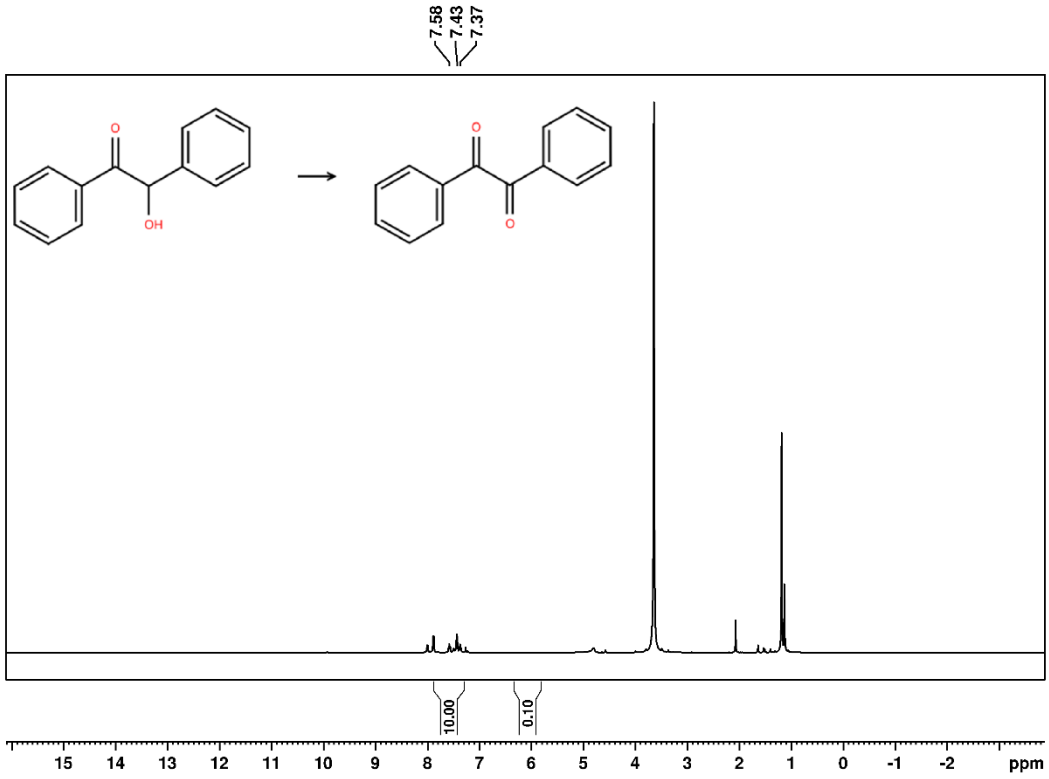

Figure 16 NMR spectrum for the catalytic oxidation of benzoin showing complete disappearance of the benzoin proton between 5.8 and 6.0 ppm.

Benzoin showed the clearest conversion, and that outcome is plausible for a vanadium-containing catalyst, because vanadium sites are well known to support oxygen-transfer and alcohol oxidation chemistry. A complete conversion here suggests that the catalyst was sufficiently active for a relatively favourable substrate, even if it was less effective for the other alcohols and alkene substrates.[56,58]

The better performance with benzoin may reflect the fact that it is more readily oxidized than simple benzylic alcohols in some heterogeneous systems, particularly when the catalyst contains accessible redox centres. It may also indicate that once the substrate is adsorbed within or near the active site, oxidation proceeds efficiently without requiring extensive pore diffusion or highly precise site geometry. At the same time, the contrast between benzoin and the less reactive substrates highlights the need to improve catalyst uniformity and access if broader substrate scope is desired.[56,59]

4.2.6 Implications for Catalyst Design

Overall, the oxidation results are best interpreted as a function of both catalyst identity and structural quality. The results establish that vanadium-containing MOFs can be highly effective oxidation catalysts; however, this performance is strictly contingent upon the framework providing accessible, stable, and uniform metal sites. The same substrate-dependent catalytic activity was observed for all the MOFs used: BM0, BM12 and BMAl. The observed substrate-dependent activity supports this view: easier-to-oxidize substrates, such as benzoin, achieved complete conversion, whereas more demanding substrates requiring higher activation energy or precise geometric constraints showed only partial conversion. This variation suggests that while the redox-active vanadium centres are intrinsically capable of catalysing these transformations, the lack of long-range order, as indicated by our PXRD results, likely introduces a heterogeneous distribution of active sites.

In this context, the more reactive substrates can access and proceed on even the less-ordered or defect-rich sites, while the challenging substrates remain inhibited by the lack of well-defined, accessible channels or by the presence of amorphous, non-catalytic vanadium oxide phases. Consequently, improving framework crystallinity is likely the critical factor for achieving high performance across a broader scope of challenging oxidation reactions.

5 Conclusion

Overall, this study shows that direct crystallization of MIL-100(V) from vanadium precursors such as $VOSO_4 \cdot 5H_2O$ and $V(acac)_3$ is difficult under the conditions tested, as these routes generally led to low crystallinity or competing oxide phases.

In contrast, successful pathways to vanadium-containing materials possessing the MIL-100 morphology were the bimetallic synthesis strategies. Specifically, vanadium incorporation into pre-formed MIL-100(Al) frameworks, synthesis of MIL-100(Fe) in situ with $VOSO_4 \cdot 5H_2O$, and the modified bimetallic method using $VOSO_4 \cdot 5H_2O$, prepared without the addition of a secondary metal source, proved effective. The room-temperature synthesis route using $VOSO_4 \cdot 5H_2O$ is particularly significant, as it provides a greener, less energy-intensive pathway to a vanadium-containing MIL-100 phase without requiring VCl_3 or harsh hydrothermal conditions.

Characterization data confirm these findings: PXRD patterns of direct synthesis products lacked the expected framework reflections, whereas samples obtained through bimetallic synthesis strategies retained the characteristic MIL-100 topology. FTIR and TGA results further support the successful formation of these MOF-like materials, and XRF analysis confirmed the effective incorporation of vanadium in the bimetallic MOF samples.

While the vanadium-containing materials were inactive for CO_2 cycloaddition, they demonstrated clear redox activity in oxidation reactions. The complete conversion of benzoin, compared to the partial conversion of other substrates, highlights that while the materials possess functional redox-active sites, their performance is strongly dictated by the crystallinity and accessibility of those sites. Ultimately, this study establishes that while direct crystallization of vanadium-based MIL-100 remains an unmet challenge, room-temperature bimetallic synthesis using $VOSO_4 \cdot 5H_2O$ offers a viable and sustainable alternative for producing vanadium-modified MIL-100 materials for catalytic applications.

References

1. Fukurawa H, Cordova KE, O'Keeffe M, Yaghi OM. The Chemistry and Applications of Metal-Organic Frameworks. *Science*. (341). doi:10.1126/science.1230444
2. Zhong G, Liu D, Zhang J. Applications of Porous Metal–Organic Framework MIL-100(M) (M = Cr, Fe, Sc, Al, V). *Cryst Growth Des*. 2018;18(12):7730-7744. doi:10.1021/acs.cgd.8b01353
3. Li D, Yadav A, Zhou H, Roy K, Thanasekaran P, Lee C. Advances and Applications of Metal-Organic Frameworks (MOFs) in Emerging Technologies: A Comprehensive Review. *Glob Chall*. 2024;8(2):2300244. doi:10.1002/gch2.202300244
4. Dhakshinamoorthy A, Alvaro M, Garcia H. Metal–organic frameworks as heterogeneous catalysts for oxidation reactions. *Catal Sci Technol*. 2011;1(6):856. doi:10.1039/c1cy00068c
5. Hall JN, Bollini P. Metal–Organic Framework MIL-100 Catalyzed Acetalization of Benzaldehyde with Methanol: Lewis or Brønsted Acid Catalysis? *ACS Catal*. 2020;10(6):3750-3763. doi:10.1021/acscatal.0c00399
6. Eddaoudi M, Kim J, Rosi N, et al. Systematic Design of Pore Size and Functionality in Isoreticular MOFs and Their Application in Methane Storage. *Science*. 2002;295(5554):469-472. doi:10.1126/science.1067208
7. Férey G, Mellot-Draznieks C, Serre C, et al. A chromium terephthalate-based solid with unusually large pore volumes and surface area. *Science*. 2005;309(5743):2040-2042. doi:10.1126/science.1116275
8. Ahmed HE, Albolkany MK, El-Khouly ME, El-Moneim AA. Tailoring MIL-100(Fe)-derived catalyst for controlled carbon dioxide conversion and product selectivity. *RSC Adv*. 2024;14(20):13946-13956. doi:10.1039/D4RA01772B
9. Volkringer C, Popov D, Loiseau T, et al. Synthesis, Single-Crystal X-ray Microdiffraction, and NMR Characterizations of the Giant Pore Metal-Organic Framework Aluminum Trimesate MIL-100. *Chem Mater*. 2009;21(24):5695-5697. doi:10.1021/cm901983a

10. Delgado-Marín JJ, Narciso J, Ramos-Fernández EV. Effect of the Synthesis Conditions of MIL-100(Fe) on Its Catalytic Properties and Stability under Reaction Conditions. *Materials*. 2022;15(18):6499. doi:10.3390/ma15186499
11. Idrees M, Mastronardo E, Piperopoulos E, Milone C, Calabrese L. Impact of HF-Free Synthesis Modification on Purity and Adsorption Performances of MOF MIL-100(Fe) for Gas Capture and Energy Storage Applications. *Appl Sci*. 2025;15(11):6097. doi:10.3390/app15116097
12. Souza BE, Tan JC. Mechanochemical approaches towards the *in situ* confinement of 5-FU anti-cancer drug within MIL-100 (Fe) metal–organic framework. *CrystEngComm*. 2020;22(27):4526-4530. doi:10.1039/D0CE00638F
13. Horcajada P, Surblé S, Serre C, et al. Synthesis and catalytic properties of MIL-100(Fe), an iron(III) carboxylate with large pores. *Chem Commun*. 2007;(27):2820-2822. doi:10.1039/B704325B
14. Vimont A, Goupil JM, Lavalley JC, et al. Investigation of Acid Sites in a Zeotypic Giant Pores Chromium(III) Carboxylate. *J Am Chem Soc*. 2006;128(10):3218-3227. doi:10.1021/ja056906s
15. Yang Q, Wiersum AD, Llewellyn PL, Guillerm V, Serre C, Maurin G. Functionalizing porous zirconium terephthalate UiO-66(Zr) for natural gas upgrading: a computational exploration. *Chem Commun*. 2011;47(34):9603. doi:10.1039/c1cc13543k
16. Horcajada P, Serre C, Maurin G, et al. Flexible Porous Metal-Organic Frameworks for a Controlled Drug Delivery. *J Am Chem Soc*. 2008;130(21):6774-6780. doi:10.1021/ja710973k
17. Reinsch H, Stock N. Formation and characterisation of Mn-MIL-100. *CrystEngComm*. 2013;15(3):544-550. doi:10.1039/C2CE26436F
18. Shi J, Hei S, Liu H, et al. Synthesis of MIL-100(Fe) at Low Temperature and Atmospheric Pressure. Gattuso G, ed. *J Chem*. 2013;2013(1):792827. doi:10.1155/2013/792827
19. Lieb A, Leclerc H, Devic T, et al. MIL-100(V) – A mesoporous vanadium metal organic framework with accessible metal sites. *Microporous Mesoporous Mater*. 2012;157:18-23. doi:10.1016/j.micromeso.2011.12.001

20. Fang Y, Yang Z, Li H, Liu X. MIL-100(Fe) and its derivatives: from synthesis to application for wastewater decontamination. *Environ Sci Pollut Res*. 2020;27(5):4703-4724. doi:10.1007/s11356-019-07318-w
21. Lisníková S, Novák P. Systematic Study on MIL-100(Fe) Synthesis Conditions to Enhance Its Properties as a Green Material for CO_2 Capture. *ACS Omega*. 2025;10(30):33461-33470. doi:10.1021/acsomega.5c03761
22. Le VN, Nguyen VC, Nguyen HT, et al. Facile synthesis of bimetallic MIL-100(Fe, Al) for enhancing CO2 Adsorption performance. *Microporous Mesoporous Mater*. 2023;360:112716. doi:10.1016/j.micromeso.2023.112716
23. Wang HH, Hou L, Li YZ, Jiang CY, Wang YY, Zhu Z. Porous MOF with Highly Efficient Selectivity and Chemical Conversion for CO_2. *ACS Appl Mater Interfaces*. 2017;9(21):17969-17976. doi:10.1021/acsami.7b03835
24. Gómez-Pozuelo G, Cabello CP, Opanasenko M, Horáček M, Čejka J. Superior Activity of Isomorphously Substituted MOFs with MIL-100(M=Al, Cr, Fe, In, Sc, V) Structure in the Prins Reaction: Impact of Metal Type. *ChemPlusChem*. 2017;82(1):152-159. doi:10.1002/cplu.201600456
25. Lyu P, Maurin G. Mechanistic Insight into the Catalytic NO Oxidation by the MIL-100 MOF Platform: Toward the Prediction of More Efficient Catalysts. *ACS Catal*. 2020;10(16):9445-9450. doi:10.1021/acscatal.0c02219
26. Kaushal S, Kaur G, Kaur J, Singh PP. First transition series metal–organic frameworks: synthesis, properties and applications. *Mater Adv*. 2021;2(22):7308-7335. doi:10.1039/D1MA00719J
27. Zhu J, Chen X, Thang AQ, et al. Vanadium-based metal-organic frameworks and their derivatives for electrochemical energy conversion and storage. *SmartMat*. 2022;3(3):384-416. doi:10.1002/smm2.1091
28. Crans DC, Smee JJ, Gaidamauskas E, Yang L. The Chemistry and Biochemistry of Vanadium and the Biological Activities Exerted by Vanadium Compounds. *Chem Rev*. 2004;104(2):849-902. doi:10.1021/cr020607t
29. Hou Y, Mao H, Xu L. MIL-100(V) and MIL-100(V)/rGO with various valence states of vanadium ions as sulfur cathode hosts for lithium-sulfur batteries. *Nano Res*. 2017;10(1):344-353. doi:10.1007/s12274-016-1326-0

30. Aureliano M, Crans DC. Decavanadate (V 10 O 28 6 -) and oxovanadates: Oxometalates with many biological activities. *J Inorg Biochem*. 2009;103(4):536-546. doi:10.1016/j.jinorgbio.2008.11.010

31. Jamali MA, Arvani A, Amini MM. Vanadium Containing Metal-organic Frameworks as Highly Efficient Catalysts for the Oxidation of Refractory Aromatic Sulfur Compounds. *ChemCatChem*. 2021;13(1):293-303. doi:10.1002/cctc.202001327

32. Loiseau T, Serre C, Huguenard C, et al. A Rationale for the Large Breathing of the Porous Aluminum Terephthalate (MIL-53) Upon Hydration. *Chem – Eur J*. 2004;10(6):1373-1382. doi:10.1002/chem.200305413

33. Barthelet K, Adil K, Millange F, Serre C, Riou D, Férey G. Synthesis, structure determination and magnetic behaviour of the first porous hybrid oxyfluorinated vanado(III)carboxylate: MIL-71 or $V^{iii}_2 (OH)_2 F_2 \{O_2 C\text{-}C_6 H_4 \text{-}CO_2\} \cdot H_2 O$. *J Mater Chem*. 2003;13(9):2208-2212. doi:10.1039/B306852H

34. Souza BE, Möslein AF, Titov K, Taylor JD, Rudić S, Tan JC. Green Reconstruction of MIL-100 (Fe) in Water for High Crystallinity and Enhanced Guest Encapsulation. *ACS Sustain Chem Eng*. 2020;8(22):8247-8255. doi:10.1021/acssuschemeng.0c01471

35. Livage J. Synthesis of polyoxovanadates via “chimie douce.” *Coord Chem Rev*. 1998;178-180:999-1018. doi:10.1016/S0010-8545(98)00105-2

36. Zavalij PY, Whittingham MS. Structural chemistry of vanadium oxides with open frameworks. *Acta Crystallogr B*. 1999;55(5):627-663. doi:10.1107/S0108768199004000

37. Riou-Cavellec M, Sanselme M, Férey G. Hybrid open frameworks: synthesis, structure and thermal behaviour of MIL-26, a new three-dimensional vanadium(iv) ethylcarboxyphosphonate Na[VIVO(O3P(CH2)2CO2)]·2H2O. *J Mater Chem*. 2000;10(3):745-748. doi:10.1039/a909870d

38. Brozek CK, Dincă M. Cation exchange at the secondary building units of metal–organic frameworks. *Chem Soc Rev*. 2014;43(16):5456-5467. doi:10.1039/C4CS00002A

39. Botas JA, Calleja G, Sánchez-Sánchez M, Orcajo MG. Cobalt Doping of the MOF-5 Framework and Its Effect on Gas-Adsorption Properties. *Langmuir*. 2010;26(8):5300-5303. doi:10.1021/la100423a

40. Lu L, Chen Q, Zhang Y, et al. Room-temperature synthesis of V-doped MIL-100(Fe) bimetallic MOF with superior antibiotics removal performance through the synergistic effect from photocatalysis and Fenton reaction. *J Adv Ceram*. 2025;14(6):9221081. doi:10.26599/JAC.2025.9221081
41. Selbin J. The Chemistry of Oxovanadium(IV). *Chem Rev*. 1965;65(2):153-175. doi:10.1021/cr60234a001
42. Cavka JH, Jakobsen S, Olsbye U, et al. A New Zirconium Inorganic Building Brick Forming Metal Organic Frameworks with Exceptional Stability. *J Am Chem Soc*. 2008;130(42):13850-13851. doi:10.1021/ja8057953
43. Taddei M, Costantino F, Marmottini F, Comotti A, Sozzani P, Vivani R. The first route to highly stable crystalline microporous zirconium phosphonate metal–organic frameworks. *Chem Commun*. 2014;50(94):14831-14834. doi:10.1039/C4CC06223J
44. Jhung SH, Lee J -H., Yoon JW, Serre C, Férey G, Chang J -S. Microwave Synthesis of Chromium Terephthalate MIL-101 and Its Benzene Sorption Ability. *Adv Mater*. 2007;19(1):121-124. doi:10.1002/adma.200601604
45. Klinowski J, Almeida Paz FA, Silva P, Rocha J. Microwave-Assisted Synthesis of Metal–Organic Frameworks. *Dalton Trans*. 2011;40(2):321-330. doi:10.1039/C0DT00708K
46. Tranchemontagne DJ, Hunt JR, Yaghi OM. Room temperature synthesis of metal-organic frameworks: MOF-5, MOF-74, MOF-177, MOF-199, and IRMOF-0. *Tetrahedron*. 2008;64(36):8553-8557. doi:10.1016/j.tet.2008.06.036
47. Walton RI, O'Hare D. An in Situ Energy-Dispersive X-ray Diffraction Study of the Hydrothermal Crystallization of Zeolite A. 2. Effect of Deuteration on Crystallization Kinetics. *J Phys Chem B*. 2001;105(1):91-96. doi:10.1021/jp002712h
48. Millange F, Serre C, Férey G. Synthesis, structure determination and properties of MIL-53as and MIL-53ht: the first Criii hybrid inorganic–organic microporous solids: Criii(OH)·{O2C–C6H4–CO2}·{HO2C–C6H4–CO2H}xElectronic supplementary information (ESI) available: crystal data, atomic coordinates and metrical parameters for MIL-53as and MIL-53ht. See

http://www.rsc.org/suppdata/cc/b2/b201381a/. *Chem Commun*. 2002;(8):822-823. doi:10.1039/b201381a

49. Choi KM, Jeon HJ, Kang JK, Yaghi OM. Heterogeneity within Order in Crystals of a Porous Metal–Organic Framework. *J Am Chem Soc*. 2011;133(31):11920-11923. doi:10.1021/ja204818q
50. Cliffe MJ, Wan W, Zou X, et al. Correlated defect nanoregions in a metal–organic framework. *Nat Commun*. 2014;5(1):4176. doi:10.1038/ncomms5176
51. Steenhaut T, Hermans S, Filinchuk Y. Green synthesis of a large series of bimetallic MIL-100(Fe,M) MOFs. *New J Chem*. 2020;44(10):3847-3855. doi:10.1039/D0NJ00257G
52. Stock N, Biswas S. Synthesis of Metal-Organic Frameworks (MOFs): Routes to Various MOF Topologies, Morphologies, and Composites. *Chem Rev*. 2012;112(2):933-969. doi:10.1021/cr200304e
53. How does XRF work? Accessed April 21, 2026. https://www.bruker.com/en/products-and-solutions/elemental-analyzers/xrf-spectrometers/how-does-xrf-work.html
54. Abid HR, Azhar MR, Iglauer S, Rada ZH, Al-Yaseri A, Keshavarz A. Physicochemical characterization of metal organic framework materials: A mini review. *Heliyon*. 2024;10(1):e23840. doi:10.1016/j.heliyon.2023.e23840
55. Embrechts H, Kriesten M, Hoffmann K, Peukert W, Hartmann M, Distaso M. Elucidation of the Formation Mechanism of Metal–Organic Frameworks via in-Situ Raman and FTIR Spectroscopy under Solvothermal Conditions. *J Phys Chem C*. 2018;122(23):12267-12278. doi:10.1021/acs.jpcc.8b02484
56. Otake K ichi, Cui Y, Buru CT, Li Z, Hupp JT, Farha OK. Single-Atom-Based Vanadium Oxide Catalysts Supported on Metal–Organic Frameworks: Selective Alcohol Oxidation and Structure–Activity Relationship. *J Am Chem Soc*. 2018;140(28):8652-8656. doi:10.1021/jacs.8b05107
57. Kim A, Ahn S, Yoon T, Notestein JM, Farha OK, Bae Y. Fast Cyclohexane Oxidation Under Mild Reaction Conditions Through a Controlled Creation of Redox-Active Fe(II/III) Sites in a Metal–Organic Framework. *ChemCatChem*. 2019;11(22):5650-5656. doi:10.1002/cctc.201901050

58. Sutradhar M, Marques G, Soliman MMA, et al. Vanadium(V) complexes supported on porous MIL-100(Fe) as catalysts for the selective oxidation of toluene. *Microporous Mesoporous Mater*. 2022;341:112091. doi:10.1016/j.micromeso.2022.112091

59. Dhakshinamoorthy A, López-Francés A, Navalon S, Garcia H. Porous Metal Organic Frameworks as Multifunctional Catalysts for Cyclohexane Oxidation. *ChemCatChem*. 2022;14(22):e202201036. doi:10.1002/cctc.202201036

60. Hacıefendioğlu D, Tuncel A. Switching of selectivity from benzaldehyde to benzoic acid using MIL-100(V) as a heterogeneous catalyst in aerobic oxidation of benzyl alcohol. *Catal Sci Technol*. 2024;14(22):6524-6536. doi:10.1039/D4CY00832D

61. Mitran G, Neaţu F, Pavel OD, Trandafir MM, Florea M. Behavior of Molybdenum–Vanadium Mixed Oxides in Selective Oxidation and Disproportionation of Toluene. *Materials*. 2019;12(5):748. doi:10.3390/ma12050748